ACS OMEGA

http://pubs.acs.org/journal/acsodf

Article

In Silico-Guided Rational Drug Design and Semi-synthesis of C(2)-Functionalized Huperzine A Derivatives as Acetylcholinesterase Inhibitors

Shisanupong Anukanon, Pornkanok Pongpamorn, Wareepat Tiyabhorn, Jaruwan Chatwichien, Worawat Niwetmarin, Richard B. Sessions, Somsak Ruchirawat, and Nopporn Thasana*

Cite This: *ACS Omega* 2021, 6, 19924−19939

Read Online

ACCESS | Metrics & More | Article Recommendations | Supporting Information

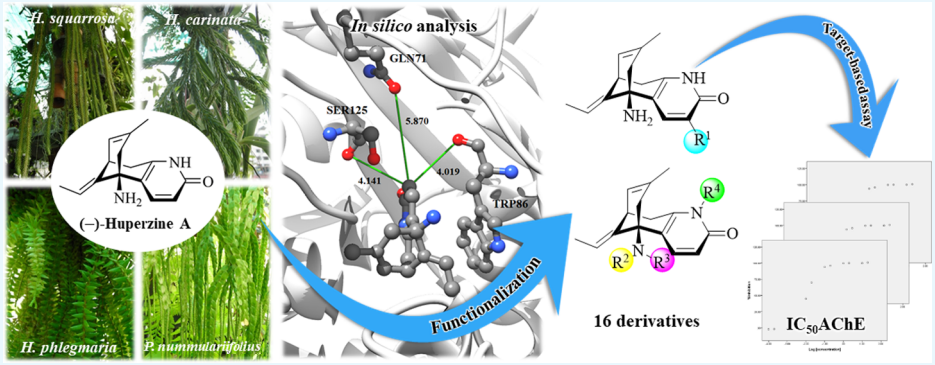

ABSTRACT: Huperzine A (**1**, Hup A), a lycodine-type *Lycopodium* alkaloid isolated from Thai clubmosses *Huperzia squarrosa* (G. Forst.) Trevis., *H. carinata* (Desv. ex. Poir.) Trevis., *H. phlegmaria* (L.), and *Phlegmariurus nummulariifolius* (Blume) Chambers (Lycopodiaceae), exerts inhibitory activity on acetylcholinesterase, a known target for Alzheimer's disease therapy. This study investigated the structure−activity relationship of C(2)-functionalized and *O*- or *N*-methyl-substituted huperzine A derivatives. *In silico*-guided screening was performed to search for potential active compounds. Molecular docking analysis suggested that substitution at the C(2) position of Hup A with small functional groups could enhance binding affinity with AChE. Consequently, 12 C(2)-functionalized and four *O*- or *N*-methyl-substituted compounds were semi-synthesized and evaluated for their *ee*AChE and *eq*BChE inhibitory activities. The result showed that 2-methoxyhuperzine A (**10**) displayed moderate to high *ee*AChE inhibitory potency (IC_{50} = 0.16 μM) with the best selectivity over *eq*BChE (selectivity index = 3633). Notably, this work showed a case of which computational analysis could be utilized as a tool to rationally screen and design promising drug molecules, getting rid of impotent molecules before going more deeply on labor-intensive and time-consuming drug discovery and development processes.

INTRODUCTION

Alzheimer's disease (AD), a dementia-related neurodegenerative brain disorder, is characterized by progressive cognitive impairment according to increments in atrophy or loss of neurons and synapse interneurons.[1] AD ranks in the top-five leading causes of global disability-adjusted life-years in patients aged 75 years and older.[2] Alzheimer's Disease International estimates that there are over 50 million people globally suffering from dementia and the number tends to increase to 152 million by 2050.[3] The characteristic pathologic hallmark of AD relates to cholinergic neuronal death in basal forebrain, neocortex, and hippocampus regions caused by deposition of amyloid-beta (Aβ) plaque and neurofibrillary tangle (NFT) in the brain.[4]

Acetylcholinesterase (AChE) is an essential enzyme that plays a key role in controlling the acetylcholine (ACh) neurotransmitter level, affecting cholinergic neurotransmission.[5] Boosting the level of ACh by AChE inhibitors is an effective symptomatic treatment of mild to moderate AD, approved by USFDA.[6] However, in advanced stages of AD, the use of AChE inhibitors is limited due to peripheral cholinergic side effects caused by nonselective inhibition of butyrylcholinesterase (BChE).[7,8] Thus to improve the efficacy and safety of symptomatic AD treatment, the development of central nervous system-selective AChE inhibitors without peripheral side effects is crucial.

Received: June 2, 2021
Accepted: July 16, 2021
Published: July 26, 2021

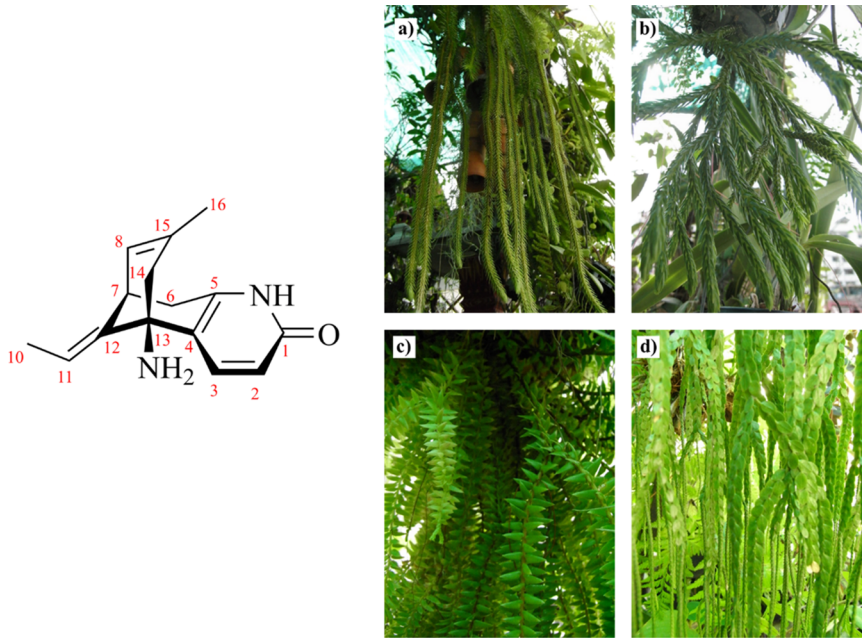

Figure 1. Structure of (−)-huperzine A (**1**) and club mosses (a) *H. squarrosa*, (b) *H. carinata*, (c) *H. phlegmaria*, and (d) *P. nummulariifolius*.

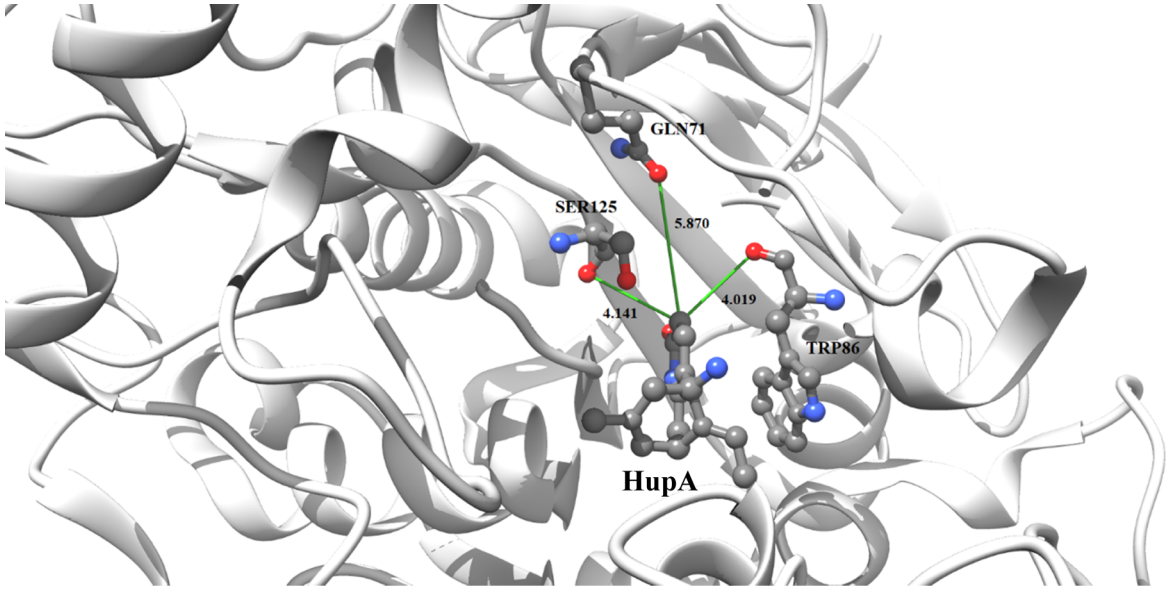

Figure 2. Molecular docking of HupA with AChE (4EY5) from BUDE and Sire Waterswap.

(−)-Huperzine A (HupA (**1**), Figure 1) is a lycodine-type *Lycopodium* alkaloid that was first isolated from Chinese clubmoss *Huperzia serrata* (family Lycopodiaceae). HupA is a potent inhibitor of AChE (IC_{50} = 0.02 μM toward *h*AChE)[9] and has been used (as a dietary supplement) to treat mild AD.[10] Although clinical studies still showed ambiguous results on the improvement of cognitive function in AD patients,[11,12] the core structure of HupA is a promising lead moiety, which can be derivatized for the development of AChE inhibitors with improved selectivity and efficacy. In our recent studies, (−)-HupA (**1**) was isolated from alkaloid-rich fractions clubmosses *Huperzia squarrosa* (G. Forst.) Trevis., *H. carinata* (Desv. ex. Poir.) Trevis., *H. phlegmaria* (L.), and *Phlegmariurus nummulariifolius* (Blume) Chambers (Lycopodiaceae) in large quantities.[13−15] With HupA in hand, chemical modifications were performed on the pyridone ring moiety by *in silico*-guided screening for potential active compounds as AChE inhibitors.

Our preliminary docking was carried out to visualize the key interactions between HupA and human AChE by using Bristol University Docking Engine (BUDE) and Sire Waterswap molecular simulation. Using the BUDE, HupA was docked into the crystal structures of recombinant human AChE (*h*AChE) in all three forms: *h*AChE in the apo state (PDB ID: 4EY4), *h*AChE complexing with HupA (PDB ID: 4EY5), and *h*AChE complexing with donepezil (PDB ID: 4EY7). BUDE managed to dock HupA into only the two forms of *h*AChE, 4EY4 and 4EY7, but it cannot re-dock HupA into the original *h*AChE in complex with HupA form (4EY5) (see Table S1, Supporting Information), which indicated that force field parameters and the binding free energy equation of BUDE were limited to analyze molecular docking accurately.[16] This led us to use the

https://doi.org/10.1021/acsomega.1c02875
ACS Omega 2021, 6, 19924−19939

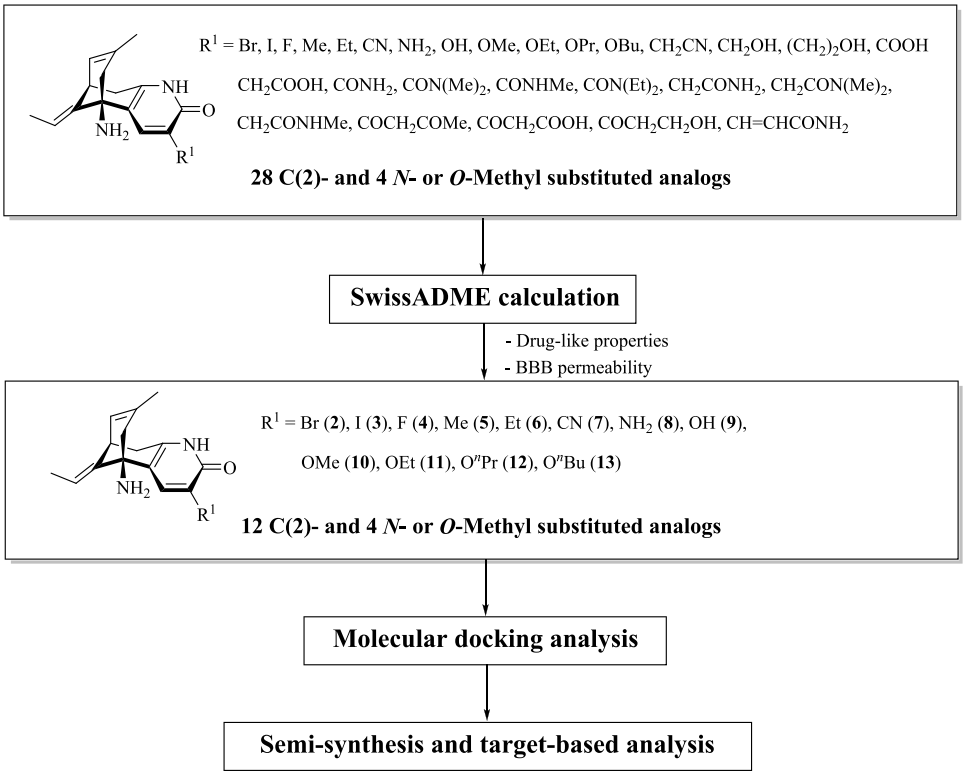

Figure 3. Design strategy for novel C(2) HupA derivatives targeting AChE.

AutoDock software for docking instead of BUDE, which is capable to re-dock HupA into original *h*AChE of 4EY5. This showed that the pyridone ring of HupA was positioned in the space between Ser125, Gln71, and Trp86 of the catalytic anionic site (CAS) of the crystallized structure of *h*AChE (4EY5) with distances of 4.141, 5.870, and 4.019 Å, respectively (Figure 2).[17] These results suggested that the substitution at C(2) of HupA could enhance binding affinity with AChE. Though there are previous reports on derivatization of HupA for AChE inhibition, including modifications at the exocyclic ethylidene group,[18] the pyridone ring,[19] the primary amine,[9,20] and the C(6) methylene position,[21−24] to the best of our knowledge, C(2) modification has not been investigated. Here, we report (i) the rational design of C(2)-functionalized HupA analogs guided by *in silico* studies (molecular docking and pharmacokinetic properties prediction); (ii) the semi-synthesis of the selected C(2)-functionalized HupA analogs; (iii) *in vitro* inhibitory activity of these novel analogs on electric eel AChE (*ee*AChE) and equine serum BChE (*eq*BChE); and (iv) structure−activity relationship (SAR) analysis of the C(2) HupA analogs described in this paper.

RESULTS AND DISCUSSION

***In Silico*-Guided Rational Drug Design.** The C(2) functionalization of HupA was designed to enhance molecular interactions of the HupA derivatives with AChE. Twenty-eight molecules, including C(2)-functionalized and *O*- or *N*-methyl-substituted HupA analogs, were subjected to SwissADME database (http://www.swissadme.ch/) to screen for drug-like characteristics and associated pharmacokinetic properties. Among this group, 12 C(2)-functionalized and four *O*- or *N*-methyl-substituted HupA analogs met the criteria of Lipinski's rules and blood−brain barrier (BBB) permeability (Figure 3). Molecular docking studies of these selected HupA derivatives (with C(2) substituents including halogens, small alkyl groups, hydroxyl, amino, nitrile, and small alkoxy groups) were then performed using Autodock software.[25,26] As shown in Table 1, C(2) analogs **5**, **6**, **8**, **9**, and **10** yielded lower binding free energies with AChE than that determined for the parent compound **1**.

Physicochemical Properties. The calculated physiochemical properties of the preselected HupA derivatives, such as the number of H-bond acceptors (HBA), number of H-bond donors (HBD), number of rotatable bonds (RB), topological polar surface area (*t*PSA), and calculated *n*-octanol/water partition coefficient (*c*LogP) were predicted, as shown in Table 2. The results demonstrated that most derivatives fell within the scope of Lipinski's rule of five except parent compound **1** and HupA analogs **7**−**10** where *c*LogP values were not within the orally available drug range.[27] For blood−brain barrier permeability, the logarithm of the brain to blood concentration ratio (log BB) was calculated by using Clark's model to determine the characteristic of the passages of the HupA derivatives through the BBB.[28] The predicted log BB values of all derivatives were greater than −1, which affirmed the possibility that these derivatives could be developed into CNS drugs.[28]

Synthesis of HupA Derivatives. We focused on the use of a range of metal-catalyzed transformations based on a C(2)-halogenated variant of HupA as a synthetic entry to the C(2) analogs that had been identified by *in silico* assessment. To avoid interference by the existing (albeit very hindered) primary amine of HupA, the amino group needed to be protected.[31] Three common protecting groups including *tert*-butyloxycarbonyl (Boc), acetyl (Ac), and triflate (Tf) were chosen as our first trials to search for the suitable protecting groups (see the Supporting Information, Scheme S1).[32] When

https://doi.org/10.1021/acsomega.1c02875
ACS Omega 2021, 6, 19924−19939

Table 1. Molecular Docking Analysis of Compounds 1−17 against *h*AChE (4EY5) and *h*BChE (4XII) Using Autodock Software

	*h*AChE (4EY5)			*h*BChE (4XII)		
compound	estimated free energy of binding (kcal/mol)[a]	estimated inhibition constant, K_i (nM)[a]	H-bond interaction residues (distance in Å)[b]	estimated free energy of binding (kcal/mol)[a]	estimated inhibition constant, K_i (nM)[a]	H-bond interaction residues (distance in Å)[b]
HupA 1	−12.17	1.20	Tyr337 (2.90), Tyr133 (2.75, 3.15)	−8.08	1.20 μM	Glu197 (2.50)
2	−12.10	1.34	Tyr133 (2.92)	−9.21	177.89	
3	−10.63	16.24	Tyr133 (2.51), Gly120 (3.15)	−8.87	313.41	Asp70 (2.48), Thr120 (2.36), Tyr332 (2.99)
4	−12.00	1.62	Tyr133 (2.87)	−8.65	453.73	Glu197 (2.77)
5	−12.20	1.13	Tyr133 (2.90, 3.15)	8.33	780.19	Asp70 (2.38), Tyr332 (2.69)
6	−12.31	0.95	Tyr133 (2.78)	−8.92	290.98	
7	−10.25	30.64	Tyr133 (2.92), Tyr337 (2.84)	−8.91	296.05	
8	−12.19	1.17	Trp86 (2.98), Tyr133 (2.87)	−8.65	458.89	Tyr128 (2.43), Glu197 (2.74)
9	−12.47	0.73	Trp86 (2.91), Tyr133 (2.89)	−8.86	321.81	Tyr128 (2.43), Glu197 (2.78)
10	−12.75	0.45	Tyr133 (2.84), Glu202 (2.70)	−9.40	129.68	Glu197 (2.51)
11	−11.30	5.23	Gly120 (2.75), Tyr133 (2.64)	−8.64	468.08	Asp70 (2.36), Tyr (2.68)
12	−11.04	8.13		−8.89	302.29	Asp70 (2.49), Tyr332 (2.67)
13	−8.45	643.06		−8.77	370.76	Glu197 (2.97), His438 (2.77)
14	−12.21	1.11	Glu202 (2.53)	−8.99	258.05	Glu197 (2.65)
15	−8.39	713.34	Ser203 (2.61), His447 (3.22)	−7.29	4.50 μM	Ser198 (3.29), His438 (2.68)
16	−9.11	211.03	Gly120 (2.99)	−7.38	3.88 μM	
17	−7.63	2.56 μM		−7.55	2.91 μM	Ser79 (3.09)
donepezil[c]	−12.42	0.78	Phe295 (2.99)	−9.99	47.44	

[a]Binding free energy and inhibitory constant results obtained from AutoDock 4.2.6 software.[25] [b]Molecular docking visualization and H-bonding measurement of each compound were obtained from UCSF Chimera Molecular graphics, and analyses were performed with UCSF Chimera.[26] [c]Donepezil, a known selective AChE inhibitor.[29]

HupA was treated with acetyl chloride in the presence of pyridine, the isomerized product **19** was observed based on NMR, possibly due to *in situ* generation of HCl or acetic acid.[33] Isomerization was avoided when HupA was treated with acetic anhydride,[34] and the desired acetyl-protected HupA **18** was isolated in 64% yield. The *N*-Tf- and *N*-Boc-protected variants **20** and **21** were prepared[35,36] and isolated in 38 and 29% yields, respectively, reflecting the hindered nature of this amine moiety. The acetyl-protected variant **18** was the most suitable since the protected HupA could be prepared in moderate yield and the acetyl group is removable under basic conditions, thus mitigating any risk of acid-promoted alkene isomerization.[37] Halogenation of *N*-Ac HupA **18** was carried out under standard conditions[38,39] to give the corresponding 2-bromo and 2-iodo derivatives **22** and **23** in good yields; however, we were then unable to remove the *N*-acetamide residue (see the Supporting Information, Scheme S1).

Given the reactivity associated with pyridone toward electrophilic substitution (which would favor reaction at C(2))[40] coupled with the hindered nature of the primary amino moiety, we explored an alternative approach, avoiding *N*-protection, as shown in Scheme 1. Unprotected HupA **1** underwent smooth and efficient electrophilic halogenation to give 2-bromohuperzine A (**2**) and 2-iodohuperzine A (**3**),[38,39] which then became attractive building blocks for further functionalization *via* various types of cross-coupling reactions. 2-Fluorohuperzine A (**4**) was then prepared from iodide **3** reacting with 1-chloromethyl-4-fluoro-1,4-diazoniabicyclo[2.2.2]octane bis(tetrafluoroborate) using Pd(dppf)Cl_2 as a catalyst in THF under reflux for 96 h.[41] 2-Alkyl HupA derivatives were prepared using Kumada or Negishi cross-coupling reactions.[42,43] The reaction of iodide **3** using Negishi's method was found to be more effective, affording the methylated and ethylated analogs **5** and **6** in 69 and 86% yields, respectively. The bromo analog **2** was, however, inert under these conditions. 2-Cyanohuperzine A (**7**) was prepared in 53% yield from **3** by the L-proline-promoted Rosenmund−von Braun reaction at 120 °C.[44] The copper-catalyzed heteroarene amination of **3** gave 2-aminohuperzine A (**8**)[44] in 90% yield. Since the corresponding 2-hydroxy was observed as a byproduct,[45] these conditions were adapted to provide 2-hydroxyhuperzine A (**9**) in 64% yield using water as a hydroxide source, instead of aqueous ammonia solution. With the successful and simple synthetic methods for **8** and **9**, the 2-alkoxy-HupA derivatives (**10**−**13**) were prepared by using an alcohol as the nucleophilic component to provide **10**−**13** in fair to good yields.

In addition to the C(2) functionalization of HupA, the modification of the pyridone ring of HupA into *O*-alkyl pyridine derivatives was performed to extend the structure−activity relationship (SAR) to *O*- or *N*-methyl-substituted HupA and *O*- or *N*-unsubstituted HupA, as shown in Scheme

https://doi.org/10.1021/acsomega.1c02875
ACS Omega 2021, 6, 19924−19939

Table 2. Physiochemical Properties of Compounds 1−17

compound	MW[a]	HBA[b]	HBD[b]	RB[b]	*t*PSA[b]	*c*LogP[b]	log BB[c]
1	242.32	2	2	0	58.88	1.88	−0.45
2	321.22	2	2	0	58.88	2.53	−0.35
3	368.22	2	2	0	58.88	2.56	−0.34
4	260.31	3	2	0	58.88	2.26	−0.39
5	256.35	2	2	0	58.88	2.22	−0.39
6	270.38	2	2	1	58.88	2.55	−0.34
7	267.33	3	2	0	82.67	1.71	−0.82
8	257.34	2	3	0	84.90	1.40	−0.90
9	258.32	3	3	0	79.11	1.58	−0.79
10	272.35	3	2	1	68.11	1.88	−0.58
11	286.38	3	2	2	68.11	2.21	−0.53
12	300.40	3	2	3	68.11	2.57	−0.48
13	314.43	3	2	4	68.11	2.91	−0.43
14	256.35	3	1	1	48.14	2.50	−0.19
15	284.40	3	0	2	25.36	3.09	0.23
16	284.40	2	0	1	25.36	3.09	0.23
17	270.37	2	1	1	36.10	2.92	0.05
donepezil[d]	381.51	4	0	6	38.77	3.85	0.15
required parameters[e]	<500	<10	<5	<10	<90	2−5	>−1.00

[a]Calculated using ChemBioDraw Ultra16.0. MW: molecular weight. [b]Calculated using SwissADME (http://www.swissadme.ch/).[30] HBA: number of hydrogen acceptors; HBD: number of hydrogen donors; RB: number of rotatable bonds; *t*PSA: total polar surface area; *c*Log P: log octanol/water partition coefficient. [c]log BB = −0.0148 × *t*PSA + 0.152 × *c*LogP + 0.139.[28] [d]Donepezil, a known selective AChE inhibitor.[29] [e]Required parameters necessary to fulfill appropriate physiochemical properties as judged appropriately according to Lipinski's rules and those important for BBB permeation.[27]

Scheme 1. Synthesis of C(2)-Functionalized HupA Derivatives 2−13[a]

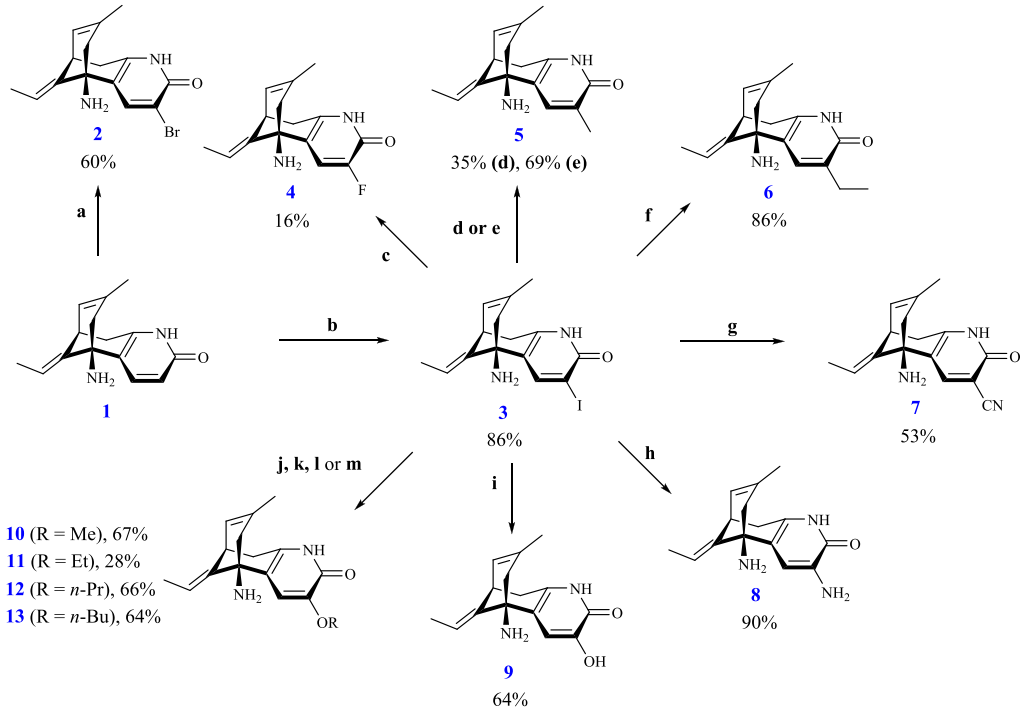

[a]Reaction conditions: (a) NBS, DCM, RT, 24 h; (b) NIS, DCM, RT, 48 h; (c) 1-chloromethyl-4-fluoro-1,4-diazoniabicyclo[2.2.2]octane bis(tetrafluoroborate), $Pd(dppf)Cl_2$, THF, reflux, 96 h; (d) CH_3MgBr, $Pd(dppf)Cl_2$, THF, reflux, 72 h; (e) $Zn(CH_3)_2$, $Pd(dppf)Cl_2$, THF, reflux, 72 h; (f) $Zn(CH_2CH_3)_2$, $Pd(dppf)Cl_2$, THF, reflux, 72 h; (g) CuCN, K_2CO_3, DMF, 120 °C, 72 h; (h) NH_3 (aq.), CuI, K_2CO_3, 140 °C, 72 h; (i) H_2O, CuI, K_2CO_3, 130 °C, 72 h; (j) MeOH, CuI, K_2CO_3, 140 °C, 72 h; (k) EtOH, CuI, K_2CO_3, 140 °C, 72 h; (l) *n*-PrOH, CuI, K_2CO_3, 140 °C, 72 h; (m) *n*-BuOH, CuI, K_2CO_3, 140 °C, 72 h.

2. By following a protocol reported by White and co-workers,[46] *O*-methyl-substituted HupA (**14**) was obtained in 46% yield by treatment of **1** with an excess of iodomethane and Ag_2CO_3 for 45 h at room temperature. When the reaction time was increased to 72 h, a mixture of *O*- or *N*-methyl-substituted HupA including *N*,*N*,*O*-trimethyl huperzine A (**15**, 19%),

https://doi.org/10.1021/acsomega.1c02875
ACS Omega 2021, 6, 19924−19939

Scheme 2. Synthesis of HupA Derivatives 14−17[a]

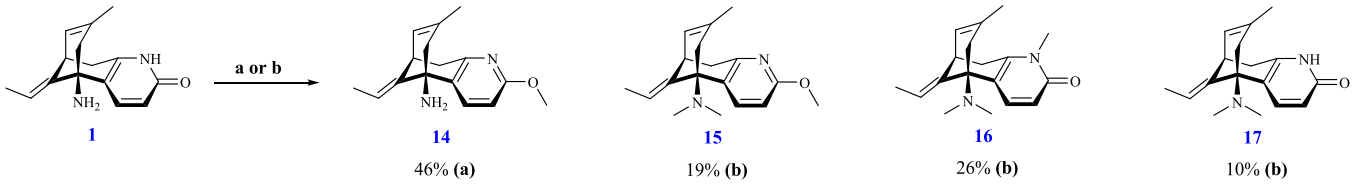

[a]Reaction conditions: (a) CH_3I, Ag_2CO_3, DCM, RT, 45 h; (b) CH_3I, Ag_2CO_3, DCM, RT, 72 h.

Table 3. *In Vitro* Inhibitory Activity of Compounds 1−17 toward Cholinesterases

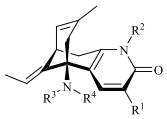

Compounds **1-13**, **16-17**

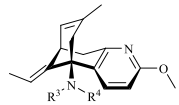

Compounds **14-15**

					cholinesterase IC_{50} (μM)[a]		
compound	R^1	R^2	R^3	R^4	*ee*AChE[b]	*eq*BChE[c]	SI[d]
1	H	H	H	H	0.03 ± 0.00	68.78 ± 03.15	2,273
2	Br	H	H	H	2.56 ± 0.17	72.29 ± 04.57	28
3	I	H	H	H	14.12 ± 0.84	325.22 ± 38.63	23
4	F	H	H	H	1.23 ± 0.01	63.998 ± 03.63	52
5	Me	H	H	H	0.35 ± 0.02	486.03 ± 29.71	1,388
6	Et	H	H	H	0.57 ± 0.09	60.39 ± 02.54	105
7	CN	H	H	H	33.88 ± 1.95	1,050.88 ± 498.89	31
8	NH_2	H	H	H	0.32 ± 0.01	524.64 ± 41.56	1,634
9	OH	H	H	H	0.53 ± 0.09	154.76 ± 04.14	293
10	OMe	H	H	H	0.16 ± 0.02	599.15 ± 49.76	3,633
11	OEt	H	H	H	0.22 ± 0.04	253.02 ± 12.24	1,154
12	O^{n}Pr	H	H	H	10.19 ± 0.50	87.27 ± 01.37	9
13	O^{n}Bu	H	H	H	109.65 ± 9.59	16.91 ± 01.23	0.2
14			H	H	3.67 ± 0.28	903.66 ± 88.20	246
15			Me	Me	n.i.	1,348.75 ± 62.31	
16		Me	Me	Me	n.i.	258.70 ± 10.81	
17			Me	Me	0.61 ± 0.02	223.57 ± 47.78	366
donepezil[e]					0.23 ± 0.05	18.00 ± 00.79	79

[a]Mean IC_{50} (μM) ± SEM, n = 3; n.i. = no inhibition. [b]AChE (EC 3.1.1.7) from electric eel. [c]BChE (EC 3.1.1.8) from horse serum. [d]Selectivity index for AChE is defined as IC_{50} (BChE)/IC_{50} (AChE). [e]Donepezil, a known selective AChE inhibitor used as a positive control.[29]

N,*N*,*N*-trimethyl huperzine A (**16**, 26%), and *N*,*N*-dimethyl huperzine A (**17**, 10%) was isolated.

***In Vitro ee*AChE and *eq*BChE Inhibition Assays.** AChE is the esterase responsible for the regulation of cholinergic transmission *via* hydrolysis of Ach, which is a primary neurotransmitter of sympathetic and parasympathetic ganglionic neurons.[8] Inhibitors of AChE can alleviate the symptoms of ACh decline by increasing cerebral cholinergic transmission at the synaptic cleft[4] and three AChE inhibitors, donepezil, rivastigmine, and galantamine, are currently approved for the treatment of AD.[47] While rivastigmine is a reversible cholinesterase inhibitor that targets both AChE and BChE,[29,48] donepezil and galantamine display better selectivity for AChE.

The *in vitro* activities of the HupA analogs **2**−**17** prepared to inhibit *ee*AChE and *eq*BChE were assessed using Ellman's method,[49] using donepezil as the reference compound. All compounds were screened at a concentration of 10 μM, and IC_{50} values were determined where inhibition was observed. The results for screening against AChE and BChE are shown in Table 3. Among C(2)-functionalized HupA derivatives, compounds **10** and **11** displayed the best *ee*AChE inhibitory activity with IC_{50} values of 0.16 and 0.22 μM, respectively, comparable to that of donepezil (IC_{50} = 0.23 μM). Although the enzyme inhibitory results did not track exactly the calculated inhibition constants reported in Table 1, all derivatives tested were less potent than the parent compound HupA **1** (IC_{50} = 0.03 μM). This observation is in accordance with many related studies of the AChE and/or BChE inhibitory activity of HupA derivatives.[50] Most of HupA analogs with substitutions at different positions on the skeleton were inactive or less active as an AChE inhibitor than HupA itself.[50] Moreover, while some analogs did show improved activities, this was also linked to a decrease in selectivity. For example, Kozikowski and co-workers[22] reported that introduction of small substituents, such as methyl or ethyl groups, at C(6) of HupA increased the inhibitory potency for AChE (IC_{50} ranging from 0.003−2.04 μM toward FBS AChE), compared to the parent compound (IC_{50} = 0.024 μM), but they also saw a reduction in selectivity in terms of the BChE/AChE inhibitory activity ratio.[22] Since 2-methoxy-HupA **10** displayed both a comparable level of activity to that of donepezil and better selectivity (selectivity index = 3633) to inhibit *ee*AChE over *eq*BChE than the HupA **1** and donepezil,

https://doi.org/10.1021/acsomega.1c02875
ACS Omega 2021, 6, 19924−19939

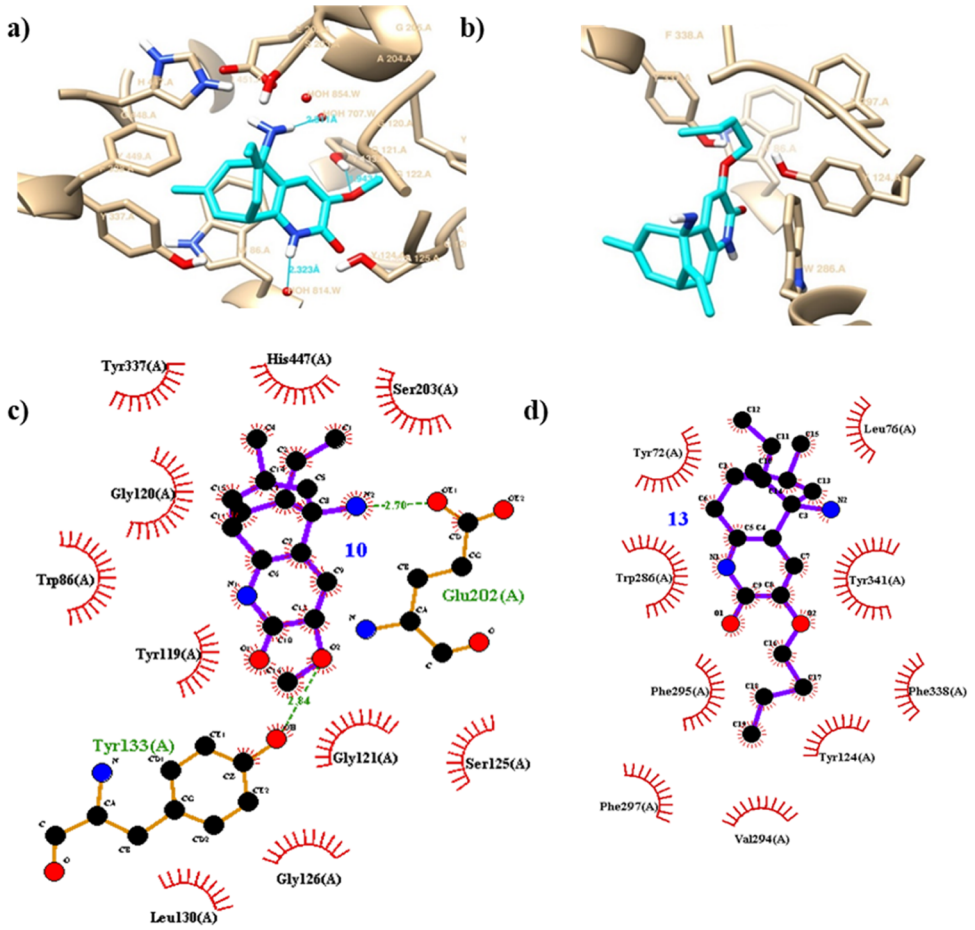

Figure 4. (a, b) Molecular docking and (c, d) binding mode analysis of compounds **10** and **13** toward AChE (4EY5).

this is a variant that could be assessed more fully for its potential for AD treatment.

Regarding the predicted physiochemical properties of HupA derivatives, as shown in Table 2, compound **10** has properties that fall within the range of the "CNS drug" compound. We observed the high log BB (>−1.0) of compound **10** that has small size and is less polar (lower number of hydrogen acceptors, lower number of hydrogen donors, and lower *t*PSA value) as parent compound **1**, suggesting that this compound could pass the BBB to alleviate the ACh level at CNS.

Structure−Activity Relationship Analysis. The relationship between the structures of C(2)-functionalized HupA derivatives and cholinesterase IC_{50} values were evaluated. Introduction of halogen substituents (compounds **2**−**4**) showed a decrease in *ee*AChE inhibitory activity. Increasing atomic radius sizes of halogen atoms also resulted in decreasing *ee*AChE inhibitory activity. For the linear alkyl side chains, IC_{50} values against *ee*AChE were elevated corresponding to the carbon numbers; from HupA **1** (0.03 ± 0.00 μM) to methy HupA **5** (0.35 ± 0.02 μM) and ethyl HupA **6** (0.57 ± 0.09 μM). Likewise, 2-methoxy-Hup A (**10**) was the most potent *ee*AChE inhibitor, compared to the other alkoxy derivatives **11**−**13** assessed, while conversely, the *n*-butoxy variant **13** preferably inhibited *eq*BChE. These observations can be explained by the bulk of the substituent at the C(2) position, preventing entry of the molecules into the AChE active site. The molecular docking and binding mode analysis of **10** and **13** confirmed the steric influence of alkoxy side chains at the C(2) position (Figure 4). The methoxy group of **10** positioned in the space between Gln69, Trp84, and Ser122 of AChE by the formation of hydrogen bonding between the 2-methoxy and hydroxyl oxygen of Tyr133 of AChE. This alignment fitted the hydrophobic region in CAS of AChE, resulting in the stronger binding to the enzymatic active site. The steric hindrance associated with the large alkyl side chain in compound **13** disrupted the binding affinity to the active site of AChE, giving the least favorable binding free energy (estimated binding free energy, −8.45 kcal/mol). Similarly, the binding mode analysis of compounds **10** and **13** within the BChE active site was also conducted, as shown in Figure 5. Both compounds occupy the space between Trp82, Tyr128, Glu167, and His438 of BChE with the same alignment as the parent compound **1**. The primary amine in compounds **10** and **13** interacted directly with carboxylate oxygen of Glu197 by H-bonding, while hydrophobic interactions were formed between the bicyclic moiety of the ligand and the indole ring of Trp82 in the same manner. On the other hand, the butoxy derivative **13** situated in the space between Trp231, Leu286, Val288, and Phe329 of BChE. The primary amine of **13** consequently interacted with the imidazole ring of His438 of BChE by H-bonding, corresponding to the lowest *in vitro* IC_{50} value for *eq*BChE activity inhibition.

The reliability of *in silico*-guided analysis was determined by correlation of estimated K_i (from docking analysis) and experimentally determined K_i (from the *in vitro* AChE inhibitory assay) values. According to the known inhibition mode of HupA, we deduce that C(2)-functionalized HupA derivatives **2**−**13** are competitive inhibitors. The experimental

https://doi.org/10.1021/acsomega.1c02875
ACS Omega 2021, 6, 19924−19939

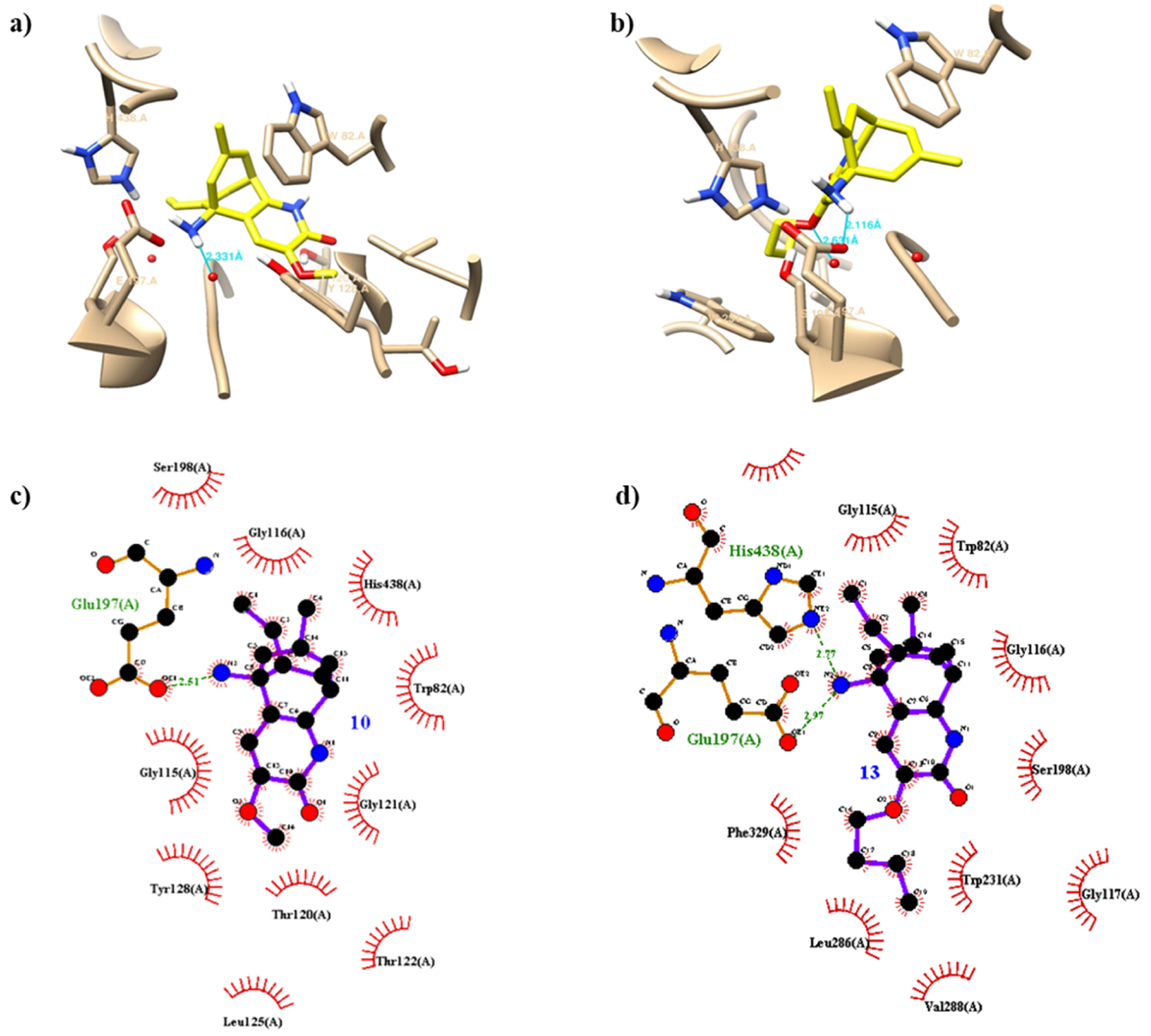

Figure 5. (a, b) Molecular docking and (c, d) binding mode analysis of compounds **10** and **13** toward BChE (4XII).

K_i values of all derivatives were calculated from *in vitro* IC_{50} values using the equations proposed by Cer and co-workers ($K_i = IC_{50}/2$).[51] Pearson's and Spearman's correlation coefficients for regression between the K_i values were also analyzed (Figure 6). The results demonstrated that the relationship between estimated K_i and experimentally determined K_i has a significant positive trend where both correlation coefficients are greater than zero (Pearson's and Spearman's coefficients of 0.96 and 0.78, respectively). The result suggested that *in silico*-guided analysis could be utilized as a reliable tool for rational drug design.

In addition to C(2)-functionalized derivatives, the structure−activity relationship of the *O*- or *N*-methyl-substituted HupA analogs was also analyzed. All *O*- or *N*-methyl-substituted HupA derivatives **14**−**17** exhibited less potent inhibitory activity on *ee*AChE than HupA **1**. The *N*- or *O*-methylated HupA derivatives, such as *N*,*N*,*O*-trimethyl HupA (**15**) and *N*,*N*,*N*-trimethyl HupA (**16**), showed no inhibition of *ee*AChE, corresponding to the *in silico* analysis that had indicated that the heteroatoms of both the pyridone ring and primary amine of HupA were necessary for binding to the active site of AChE. *N*,*N*-Dimethyl HupA (**17**) showed greater *ee*AChE inhibitory activity than the *O*-methyl HupA (**14**), suggesting that interactions involving the pyridone ring of HupA were more crucial than the amino group for AChE inhibition. Methyl substitution at the nitrogen pyridone ring of HupA has been evaluated for the AChE inhibitory activity.[18] This compound showed low potency for brain AChE inhibitory activity, similar to the activity that we observed for compound **16**. Moreover, the transformation of the pyridine ring from the pyridone ring of HupA as catechol analogs was also reported with inactivity or less activity than HupA in AChE.[24]

To evaluate the cytotoxicity of the HupA derivatives reported here and donepezil, an MTT (3-(4,5-dimethylthiazol-2-yl)-2,5-diphenyltetrazolium bromide) assay was performed. Each compound was tested at two concentrations, 10 and 100 μM, against human lung fibroblast cells (IMR90). As demonstrated in Table 4, at 10 μM concentration, all compounds failed to affect the cell proliferation. Among them (and at 100 μM), only **6**, **15**, and donepezil showed some cytotoxicity while compound **6** was still significantly less toxic than donepezil. Interestingly, we did not observe any cell toxicity for ligand **10**, which is the most promising selective inhibitor that we have identified.

https://doi.org/10.1021/acsomega.1c02875
ACS Omega 2021, 6, 19924−19939

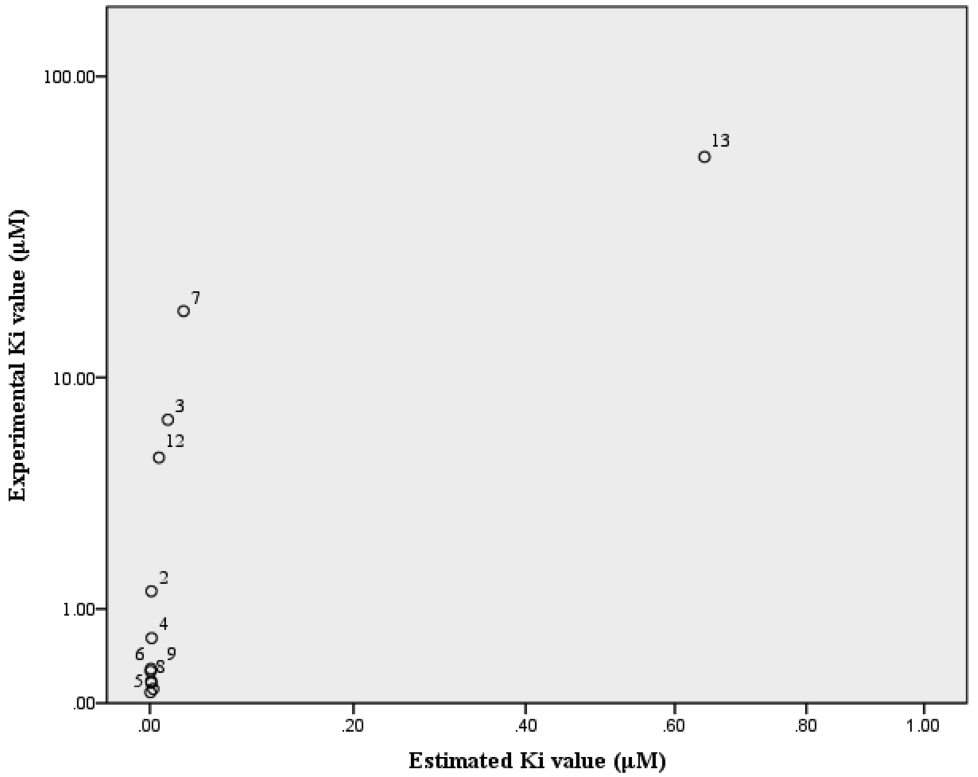

Figure 6. Correlation of the estimated K_i value according to the docking program and calculated K_i according to *in vitro* results. Correlation is significant at the $p < 0.001$ level (two-tailed).

Table 4. *In Vitro* Cytotoxicity of HupA Derivatives and Donepezil against IMR90 Cells[a]

	%cytotoxicity[b]			%cytotoxicity[b]	
compound	10 μM	100 μM	compound	10 μM	100 μM
1	n.i.	n.i.	**10**	n.i.	n.i.
2	n.i.	n.i.	**11**	n.i.	n.i.
3	n.i.	n.i.	**12**	n.i.	n.i.
4	n.i.	n.i.	**13**	n.i.	n.i.
5	n.i.	n.i.	**14**	n.i.	n.i.
6	n.i.	2.2 ± 2.4[c]	**15**	n.i.	5.5 ± 9.7
7	n.i.	n.i.	**16**	n.i.	n.i.
8	n.i.	n.i.	**17**	n.i.	n.i.
9	n.i.	n.i.	donepezil	n.i.	29.0 ± 12.5

[a]IMR90 cells were treated with each compound at the indicated concentrations for 24 h. Cell viability was determined by the MTT assay. [b]The values are shown as mean ± SEM, $n = 3$. n.i. = no inhibition. [c]Significantly different from donepezil (100 μM) with $p < 0.05$.

CONCLUSIONS

In this paper, we report the semi-synthesis of a set of novel C(2)-functionalized HupA derivatives that were designed using *in silico* binding affinity to AChE and predicted the pharmacokinetic properties. Among the variants synthesized, 2-methoxy-HupA **10** was found to be the most potent *ee*AChE inhibitor with improved selectivity over *eq*BChE, compared to HupA (~2 times) and donepezil (~46 times). In addition, using an MTT assay, ligand **10** was significantly less cytotoxic than donepezil. These results suggested the potential of ligand **10** to be further developed as an AD treatment with less peripheral side effects. The structure–activity relationship of the *O*- or *N*-methyl-substituted HupA compounds **14**–**17** was also studied. The results revealed that the nitrogen atom of the pyridone ring, rather than the primary amine of HupA, was crucial for AChE binding. The detailed structure–activity relationship analysis of HupA derivatives reported here should be useful for the future development of anti-AD drugs.

EXPERIMENTAL SECTION

Computational Analysis. *Preparation of the Structures of HupA Derivatives.* Structures of HupA and its analogs were constructed in ChemDraw Professional 16.0 followed by three-dimensional (3D) structure transformation using Chem3D Professional 10.0. All analogs were then energetically minimized by Chem3D Professional 10.0 by using the MM2 force field to avoid any steric clashes of the freely rotatable bond.

Molecular Docking of HupA Analogs into AChE. The binding free energy and inhibitory constant K_i of HupA, HupA analogs, and donepezil (as a reference compound with AChE inhibition) were docked and analyzed by using AutoDock 4.2.6 software. The crystal structures of human AChE (PDB entry: 4EY5) and BChE (PDB entry: 4XII) were prepared by removing all water molecules, any solvent, and the ligand. Each energy-minimized HupA analogs were submitted with default parameters of docking procedures. The binding site sphere for HupA derivatives interaction was defined around the catalytic site according to previous studies (Tyr72, Asp74, Trp86, Gly121, Gly122, Glu202, Ser203, Ala204, Trp236, Trp286, Phe295, Phe297, Glu334, Tyr337, Phe338, and His447 for the AChE active site and Trp82, Trp231, Phe329, and Tyr332 for the BChE active site). The Ser124 and Gln71 residues were also included to determine the free pocket space of AChE for the C(2) functional group of HupA derivatives. The molecular docking protocol was obtained from the active site of the

https://doi.org/10.1021/acsomega.1c02875
ACS Omega 2021, 6, 19924–19939

AChE and BChE with a molecular grid at 0.375 Å grid spacing. The grids were located at $x = -6.750$, $y = -6.250$, and $z = 3.389$ Å for AChE and $x = 4.302$, $y = -7.649$, and $z = -14.515$ Å for BChE. Docking results of all HupA analogs with AChE and BChE were evaluated as the best binding free energy (BE, kcal/mol) and inhibitory constant K_i from all clusters of each conformational structure. Virtual analysis of the best result of each analog was viewed and analyzed by using UCSF Chimera.[26]

Computational Pharmacokinetic Analysis. The SwissADME is a free web tool to compute the physicochemical properties of a small molecule to evaluate lead candidates of HupA analogs (http://www.swissadme.ch/index.php).[30] All analogs were submitted in the SMILES format to calculate the pharmacokinetic properties of HupA analog candidates. The physicochemical properties of SwissADME results include molecular weight (MW), number of heavy atoms, number of the rotatable bonds, number of H-bond acceptors (HA), number of H-bond donors, polar surface area (PSA), and lipophilicity were obtained.

Semi-synthesis of HupA Analogs. *General Chemistry.* The HupA (**1**) starting material was isolated from clubmosses *H. squarrosa* (G. Forst.) Trevis., *H. carinata* (Desv. ex. Poir.) Trevis., *H. phlegmaria* (L.), and *P. nummulariifolius* (Blume) Chambers (Lycopodiaceae),[13−15] and used in the semi-synthesis of *N*-protection of HupA derivatives (Scheme 2 and Scheme S1). Commercial HupA (99% purity) was purchased from Changsha Zhongren Biotechnology (Changsha City, Hunan, China) and used in the semi-synthesis of C(2)-functionalized HupA derivatives, as shown in Scheme 1. All reagents and solvents were obtained from commercial suppliers and used without further purification. The reactions were performed based on previously published procedures and monitored by thin-layer chromatography (TLC) on silica gel pre-coated aluminum plates (70−230 mesh). The TLC spots were visualized by UV light at 254 and 365 nm. The purification of all desired products was carried out by using silica gel column chromatography (70−230 mesh of SiliCycle silica gel), which provided isolated yield. ^{1}H and ^{13}C NMR spectra were collected on a Bruker AVANCE at 300 and 75 MHz, respectively. Chemical shifts (δ) were reported in parts-per-million (ppm) relative to residual solvent signals. The 1D spectra was measured in $CDCl_3$, which were referenced to 7.26 ppm for ^{1}H NMR and 77 ppm for ^{13}C NMR. High-resolution mass spectra were obtained using electron spray ionization (ESI) on a Thermo Scientific QTOF instrument.

*Formation of Compound **2** by Bromination of Huperzine A (**1**).* HupA (**1**, 0.21 mmol, 50 mg) was treated with *N*-bromosuccinimide (NBS, 0.62 mmol, 110 mg) in CH_2Cl_2 (1.0 mL) at room temperature for 24 h. The reaction mixture was quenched with H_2O (5 mL) and extracted three times with CH_2Cl_2 (5 mL). The combined organic layers were washed with sat. NaCl (5 mL), then dried over anhydrous Na_2SO_4, and concentrated under reduced pressure. The crude product was purified by flash column chromatography (4−7% v/v MeOH in CH_2Cl_2) to afford 2-bromohuperzine A (**2**, 40 mg, 60%).

*(5R,9R,E)-5-Amino-11-ethylidene-3-bromo-7-methyl-5,6,9,10-tetrahydro-5,9-methanocycloocta[b]pyridin-2(1H)-one (**2**).* Yellowish solid; m.p. 199−200 °C; $[\alpha]_D^{26}$ −135.2° (*c* 2.5, CH_3OH); R_f = 0.40 (7% v/v MeOH in CH_2Cl_2); IR (neat) ν 2927, 1638, 1610, 1549, 1457, 600 cm^{-1}; ^{1}H NMR (300 MHz, $CDCl_3$) δ_H 8.30 (s, 1H), 5.49 (q, *J* = 6.6 Hz, 1H), 5.43 (d, *J* = 6.0 Hz, 1H), 3.60−3.66 (m, 1H), 2.88 (dd, *J* = 16.5, 6.0 Hz, 1H), 2.76 (dd, *J* = 16.5, 3.0 Hz, 1H), 2.13 (d, *J* = 6.0 Hz, 2H), 1.68 (d, *J* = 6.6 Hz, 3H), 1.56 (s, 3H); ^{13}C NMR (75 MHz, $CDCl_3$) δ_C 161.4, 143.3, 142.3, 142.1, 134.1, 124.3, 124.0, 111.8, 111.74, 54.39, 49.24, 35.1, 32.8, 22.6, 12.4; (+)-HRMS (ESI) *m*/*z* calcd for $C_{15}H_{18}{}^{79}BrN_2O$ $[M + H]^+$, 321.0597; found 321.0585.

*Formation of Compound **3** by Iodination of Huperzine A (**1**).* HupA (**1**, 0.41 mmol, 100 mg) was treated with *N*-iodosuccinimide (NIS, 0.62 mmol, 139 mg) in CH_2Cl_2 (2.5 mL) at room temperature for 72 h. The reaction mixture was quenched with H_2O (10 mL) and extracted three times with CH_2Cl_2 (10 mL). The combined organic layers were washed with sat. NaCl (10 mL), then dried over anhydrous Na_2SO_4, and concentrated under reduced pressure. The crude product was purified by flash column chromatography (7% v/v MeOH in CH_2Cl_2) to afford 2-iodohuperzine A (**3**, 103 mg, 68%).

*(5R,9R,E)-5-Amino-11-ethylidene-3-iodo-7-methyl-5,6,9,10-tetrahydro-5,9-methanocycloocta[b]pyridin-2(1H)-one (**3**).* White-yellowish solid; m.p. 250−251 °C; $[\alpha]_D^{26}$ −151.0° (*c* 4.0, CH_3OH); R_f = 0.46 (7% v/v MeOH in CH_2Cl_2); IR (neat) ν 2924, 1630, 1606, 1541, 1449, 589 cm^{-1}; ^{1}H NMR (300 MHz, $CDCl_3$) δ_H 8.49 (s, 1H), 5.46 (q, *J* = 6.6 Hz, 1H), 5.41 (d, *J* = 6.0 Hz, 1H), 3.59−3.63 (m, 1H), 2.85 (dd, *J* = 18.0, 6.0 Hz, 1H), 2.73 (dd, *J* = 18, 3.0 Hz, 1H), 2.11 (s, 2H), 1.65 (d, *J* = 6.6 Hz, 3H), 1.53 (s, 3H); ^{13}C NMR (75 MHz, $CDCl_3$) δ_C 162.4, 149.1, 144.5, 142.1, 134.1, 124.6, 124.4, 111.7, 87.3, 54.3, 49.3, 35.1, 32.8, 22.7, 12.5; (+)-HRMS (ESI) *m*/*z* calcd for $C_{15}H_{18}IN_2O$ $[M + H]^+$, 369.0458; found 369.0451.

*Formation of Compound **4** by Fluorination of 2-Iodohuperzine A (**3**).* To a solution of 2-iodohuperzine A (**3**, 0.14 mmol, 50 mg) in THF (1.0 mL) were added bis(triphenylphosphine)palladium dichloride (20 mg, 4 mol %) and 1-chloromethyl-4-fluoro-1,4-diazoniabicyclo[2.2.2]-octane bis(tetrafluoroborate) (0.68 mmol, 241 mg). The mixture was heated at reflux temperature for 96 h under an Ar atmosphere. After cooling to room temperature, the reaction mixture was quenched with H_2O (10 mL) and extracted three times with CH_2Cl_2 (10 mL). The combined organic layers were washed with sat. NaCl (10 mL), then dried over anhydrous Na_2SO_4, and concentrated under reduced pressure. The crude product was purified by flash column chromatography (5% v/v MeOH in ethyl acetate) to afford 2-fluorohuperzine A (**4**, 6 mg, 16%).

*(5R,9R,E)-5-Amino-11-ethylidene-3-fluoro-7-methyl-5,6,9,10-tetrahydro-5,9-methanocycloocta[b]pyridin-2(1H)-one (**4**).* Yellowish semisolid; $[\alpha]_D^{26}$ −48.0° (*c* 1.0, CH_3OH); R_f = 0.2 (100% ethyl acetate); IR (neat) ν 2920, 1662, 1619, 1437, 1305 cm^{-1}; ^{1}H NMR (300 MHz, $CDCl_3$) δ_H 7.74 (d, *J* = 6.0 Hz, 1H), 5.49 (q, *J* = 6.0 Hz, 1H), 5.41 (d, *J* = 3.0 Hz, 1H), 3.60−3.64 (m, 1H), 2.87 (d, *J* = 18.0 Hz, 1H), 2.70 (d, *J* = 18.0 Hz, 1H), 2.13 (s, 1H), 2.11 (s, 1H), 1.69 (d, *J* = 9.0 Hz, 3H), 1.56 (s, 3H); ^{13}C NMR (75 MHz, $CDCl_3$) δ_C 158.2, 138.1, 134.26, 124.3, 121.9, 121.7, 111.8, 77.4, 54.5, 49.1, 34.8, 33.0, 29.8, 22.7, 12.5; (+)-HRMS (ESI) *m*/*z* calcd for $C_{15}H_{18}FN_2O$ $[M + H]^+$, 261.1398; found 261.1399.

*Formation of Compound **5** by Methylation of 2-Iodohuperzine A (**3**) Using the Negishi Cross-Coupling Reaction.* To a solution of 2-iodohuperzine A (**3**, 0.27 mmol, 100 mg) in THF (1.0 mL) were added bis-(triphenylphosphine)palladium dichloride (22 mg, 10 mol %) and dimethylzinc (0.81 mmol, 0.8 mL of 1 M dimethylzinc

https://doi.org/10.1021/acsomega.1c02875
ACS Omega 2021, 6, 19924−19939

in toluene solution). The resulting yellow solution was heated at reflux temperature for 72 h under an Ar atmosphere. After cooling to room temperature, the reaction mixture was quenched with methanol (1.0 mL) and *tert*-butyl methyl ether (10 mL). The resulting mixture was washed three times with water (10 mL) and sat. NaCl (10 mL), then dried over anhydrous Na_2SO_4, and concentrated under reduced pressure. The crude product was purified by flash column chromatography (7% v/v MeOH in CH_2Cl_2) to afford 2-methylhuperzine A (**5**, 46 mg, 67%).

*(5R,9R,E)-5-Amino-11-ethylidene-3,7-dimethyl-5,6,9,10-tetrahydro-5,9-methanocycloocta[b]pyridin-2(1H)-one (**5**).* Brownish solid; m.p. 83−85 °C; $[\alpha]_D^{26}$ −150.0° (*c* 3.8, CH_3OH); R_f = 0.26 (7% v/v MeOH in CH_2Cl_2); IR (neat) ν 2918, 1642, 1618, 1572, 1263 cm^{-1}; ^1H NMR (300 MHz, $CDCl_3$) δ_H 7.71 (s, 1H), 5.47 (q, *J* = 9.0 Hz, 1H), 5.41 (s, 1H), 3.55−3.65 (m, 1H), 2.87 (dd, *J* = 18.0, 3.0 Hz, 1H), 2.56 (d, *J* = 15.0, 1H), 2.14 (s, 2H), 2.12 (s, 3H), 1.67 (d, *J* = 6.0 Hz, 3H), 1.54 (s, 3H); ^{13}C NMR (75 MHz, $CDCl_3$) δ_C 165.3, 142.9, 140.0, 137.4, 134.2, 125.8, 124.4, 122.1, 110.9, 54.4, 49.2, 35.0, 33.1, 22.7, 16.5, 12.4; (+)-HRMS (ESI) *m*/*z* calcd for $C_{16}H_{21}N_2O$ $[M + H]^+$, 257.1648; found 257.1647.

*Formation of Compound **6** by Ethylation of 2-Iodohuperzine A (**3**) Using the Negishi Cross-Coupling Reaction.* To a solution of 2-iodohuperzine A (**3**, 0.27 mmol, 100 mg) in THF (1.0 mL) were added bis-(triphenylphosphine)palladium dichloride (22 mg, 10 mol %) and diethylzinc (0.81 mmol, 0.8 mL of 1 M diethylzinc in toluene solution). The resulting yellow solution was heated at reflux temperature for 72 h under an Ar atmosphere. After cooling to room temperature, the reaction mixture was quenched with methanol (1.0 mL) and *tert*-butyl methyl ether (10 mL). The resulting mixture was washed three times with water and sat. NaCl (10 mL), then dried over anhydrous Na_2SO_4, and concentrated under reduced pressure. The crude product was purified by flash column chromatography (7% v/v MeOH in CH_2Cl_2) to afford 2-ethylhuperzine A (**6**, 29 mg, 39%).

*(5R,9R,E)-5-Amino-3-ethyl-11-ethylidene-7-methyl-5,6,9,10-tetrahydro-5,9-methanocycloocta[b]pyridin-2(1H)-one (**6**).* Brownish solid; m.p. 243−244 °C; $[\alpha]_D^{26}$ −173.0° (*c* 2.0, CH_3OH); R_f = 0.31 (7% v/v MeOH in CH_2Cl_2); IR (neat) ν 2972, 1643, 1620, 1568, 1264 cm^{-1}; ^1H NMR (300 MHz, $CDCl_3$) δ_H 7.70 (s, 1H), 5.47 (q, *J* = 6.0 Hz, 1H), 5.39 (d, *J* = 3.0 Hz, 1H), 3.55−3.65 (m, 1H), 2.85 (dd, *J* = 18.0, 3.0 Hz, 1H), 2.66 (d, *J* = 18.0 Hz, 1H), 2.52 (q, *J* = 6.0 Hz, 2H), 2.19 (s, 1H), 2.10 (s, 1H), 1.67 (d, *J* = 6.0 Hz, 3H), 1.54 (s, 3H), 1.18 (t, *J* = 6.0 Hz, 3H); ^{13}C NMR (75 MHz, $CDCl_3$) δ_C 164.7, 142.6, 139.8, 135.6, 134.2, 131.7, 124.4, 122.1, 111.1, 54.5, 49.1, 35.0, 33.0, 23.4, 22.8, 13.1, 12.5; (+)-HRMS (ESI) *m*/*z* for $C_{17}H_{23}N_2O$ $[M + H]^+$, 271.1805; found 271.1805.

*Formation of Compound **7** by Cyanidation of 2-Iodohuperzine A (**3**) Using the Rosenmund−von Braun Reaction.* To a solution of 2-iodohuperzine A (**3**, 0.14 mmol, 50 mg) in DMF (3.0 mL) were added CuCN (0.68 mmol, 61 mg) and K_2CO_3 (0.41 mmol, 56 mg). The mixture was heated at 120 °C for 72 h under an Ar atmosphere. After cooling to room temperature, the reaction mixture was quenched with H_2O (10 mL) and extracted three times with CH_2Cl_2 (10 mL). The combined organic layers were washed with sat. NaCl (10 mL), then dried over anhydrous Na_2SO_4, and concentrated under reduced pressure. The crude product was purified by flash column chromatography (2−7% v/v MeOH in CH_2Cl_2) to afford 2-cyanohuperzine A (**7**, 19 mg, 53%).

*(5R,9R,E)-5-Amino-11-ethylidene-7-methyl-2-oxo-1,2,5,6,9,10-hexahydro-5,9-methanocycloocta[b]pyridine-3-carbonitrile (**7**)*

Yellowish solid; m.p. 244−245 °C; $[\alpha]_D^{26}$ −247.5° (*c* 1.6, CH_3OH); R_f = 0.46 (7% v/v MeOH in CH_2Cl_2); IR (neat) ν 2225, 1651, 1597, 1566, 1304 cm^{-1}; ^1H NMR (300 MHz, $CDCl_3$) δ_H 8.43 (s, 1H), 5.51 (q, *J* = 6.0 Hz, 1H), 5.54 (d, *J* = 6.0 Hz, 1H), 3.60−3.70 (m, 1H), 2.91 (dd, *J* = 18.0, 3.0 Hz, 1H), 2.84 (dd, *J* = 18.0, 1.5 Hz, 1H), 2.11 (s, 2H), 1.69 (d, *J* = 9.0 Hz, 3H), 1.54 (s, 3H); ^{13}C NMR (75 MHz, $CDCl_3$) δ_C 163.0, 150.9, 147.5, 141.5, 134.1, 124.5, 124.3, 116.2, 112.6, 101.3, 54.5, 49.6, 35.9, 32.6, 22.6, 12.5; (+)-HRMS (ESI) *m*/*z* for $C_{16}H_{17}N_3O$ $[M + H]^+$, 268.1444; found 268.1447.

*Formation of Compound **8** by Copper-Catalyzed Heteroarene Amination of 2-Iodohuperzine A (**3**).* 2-Iodohuperzine A (**3**, 0.14 mmol, 50 mg), copper(I) iodide (1 mg, 4 mol %), and K_2CO_3 (0.41 mmol, 56 mg) were charged in a 15 mL sealed screw-capped tube under air, and 5.0 mL of aqueous ammonia solution (*ca.* 28%) was added *via* a syringe. The sealed tube was closed tightly after purging with argon gas flow. The reaction mixture was heated at 140 °C and stirred for 72 h. After cooling to room temperature, the reaction mixture was quenched with H_2O (10 mL) and extracted three times with CH_2Cl_2 (10 mL). The combined organic layers were washed with sat. NaCl (10 mL), then dried over anhydrous Na_2SO_4, and concentrated under reduced pressure. The crude product was purified by flash column chromatography (7−15% v/v MeOH in CH_2Cl_2) to afford 2-aminohuperzine A (**8**, 32 mg, 90%).

*(5R,9R,E)-3,5-Diamino-11-ethylidene-7-methyl-5,6,9,10-tetrahydro-5,9-methanocycloocta[b]pyridin-2(1H)-one (**8**).* Yellowish solid; m.p. 82−84 °C; $[\alpha]_D^{26}$ −145.3° (*c* 1.9, CH_3OH); R_f = 0.11 (10% v/v MeOH in CH_2Cl_2); IR (neat) ν 3450, 3295, 1645, 1589, 1454 cm^{-1}; ^1H NMR (300 MHz, CD_3OD) δ_H 7.06 (s, 1H), 5.50 (q, *J* = 6.0 Hz, 1H), 5.43 (d, *J* = 3.0 Hz, 1H), 3.60−3.70 (m, 1H), 2.75 (dd, *J* = 18.0, 6.0 Hz, 1H), 2.51 (dd, *J* = 18.0, 3.0 Hz, 1H), 2.23 (s, 2H), 1.71 (d, *J* = 9.0 Hz, 3H), 1.56 (s, 3H); ^{13}C NMR (75 MHz, CD_3OD) δ_C 159.8, 142.0, 137.0, 135.0, 130.5, 125.2, 124.1, 115.1, 112.4, 55.5, 49.4, 35.4, 34.2, 22.7, 12.5; (+)-HRMS (ESI) *m*/*z* calcd for $C_{15}H_{20}N_3O$ $[M + H]^+$, 258.1601 ; found 258.1603.

*Formation of Compound **9** by Copper-Catalyzed Heteroarene Hydroxylation of 2-Iodohuperzine A (**3**).* 2-Iodohuperzine A (**3**, 0.14 mmol, 50 mg), copper(I) iodide (1 mg, 4 mol %), and K_2CO_3 (0.41 mmol, 56 mg) were charged in a 15 mL sealed screw-capped tube under air, and 5.0 mL of deionized water was added *via* a syringe. The sealed tube was closed tightly after purging with argon gas flow. The reaction mixture was heated at 140 °C and stirred for 72 h. After cooling to room temperature, the reaction mixture was quenched with H_2O (10 mL) and extracted three times with CH_2Cl_2 (10 mL). The combined organic layers were washed with sat. NaCl (10 mL), then dried over anhydrous Na_2SO_4, and concentrated under reduced pressure. The crude product was purified by flash column chromatography (7−15% v/v MeOH in CH_2Cl_2) to afford 2-hydroxyhuperzine A (**9**, 22 mg, 64%).

*(5R,9R,E)-5-Amino-11-ethylidene-3-hydroxy-7-methyl-5,6,9,10-tetrahydro-5,9-methanocycloocta[b]pyridin-2(1H)-one (**9**).* Yellowish solid; m.p. 83−85 °C; $[\alpha]_D^{26}$ −151.2° (*c* 2.5, CH_3OH); R_f = 0.14 (10% v/v MeOH in CH_2Cl_2); IR (neat) ν

https://doi.org/10.1021/acsomega.1c02875
ACS Omega 2021, 6, 19924−19939

3356, 2923, 1648, 1615, 1580, 1439 cm^{-1}; ^1H NMR (300 MHz, $(CD_3)_2SO$) δ_H 7.10 (s, 1H), 5.45 (q, J = 6.0 Hz, 1H), 5.38 (d, J = 4.5 Hz, 1H), 3.40−3.55 (m, 1H), 2.57 (dd, J = 18.0, 6.0 Hz, 1H), 2.40 (d, J = 18.0 Hz, 1H), 1.90−2.10 (m, 2H), 1.62 (d, J = 6.0 Hz, 3H), 1.49 (s, 3H); ^{13}C NMR (75 MHz, $(CD_3)_2SO$) δ_C 158.3, 144.7, 142.1, 133.5, 130.2, 124.4, 121.2, 114.7, 110.4, 53.9, 48.3, 34.1, 32.4, 22.4, 12.1; (+)-HRMS (ESI) m/z calcd for $C_{15}H_{19}N_2O_2$ $[M + H]^+$, 259.1447; found 259.1441.

Formation of Compound ***10*** *by Copper-Catalyzed Heteroarene Methoxylation of 2-Iodohuperzine A (**3**).* 2-Iodohuperzine A (**3**, 0.27 mmol, 100 mg), copper(I) iodide (2 mg, 4 mol %), and K_2CO_3 (0.81 mmol, 112 mg) were charged in a 15 mL sealed screw-capped tube under air, and 5.0 mL of methanol was added *via* a syringe. The sealed tube was closed tightly after purging with argon gas flow. The reaction mixture was heated at 140 °C and stirred for 120 h. The crude mixture was filtered through a patch of silica gel and washed with MeOH. The crude product was purified by flash column chromatography (7% v/v MeOH in ethyl acetate) to afford 2-methoxyhuperzine A (**10**, 49 mg, 66%).

*(5R,9R,E)-5-Amino-11-ethylidene-3-methoxy-7-methyl-5,6,9,10-tetrahydro-5,9-methanocycloocta[b]pyridin-2(1H)-one (**10**).* Brownish solid; m.p. 90−91 °C; $[\alpha]_D^{26}$ −89.0° (c 2.0, CH_3OH); R_f = 0.18 (7% v/v MeOH in CH_2Cl_2); IR (neat) ν 2910, 1647, 1620, 1571, 1462, 1247 cm^{-1}; ^1H NMR (300 MHz, $(CD_3)_2SO$) δ_H 7.22 (s, 1H), 5.48 (q, J = 6.0 Hz, 1H), 5.37 (d, J = 3.0 Hz, 1H), 3.83 (s, 3H), 3.47−3.53 (m, 1H), 2.55 (dd, J = 18.0, 6.0 Hz, 1H), 2.53 (d, J = 18.0 Hz, 1H), 2.05 (s, 2H), 1.61 (d, J = 6.0 Hz, 3H), 1.49 (s, 3H); ^{13}C NMR (75 MHz, $(CD_3)_2SO$) δ_C 157.0, 147.3, 142.1, 133.5, 131.7, 124.4, 120.1, 113.6, 110.4, 55.3, 54.0, 48.2, 34.0, 32.3, 22.4, 12.1; (+)-HRMS (ESI) m/z calcd for $C_{16}H_{21}N_2O_2$ $[M + H]^+$, 273.1598; found 273.1597.

Formation of Compound ***11*** *by Copper-Catalyzed Heteroarene Ethoxylation of 2-Iodohuperzine A (**3**).* 2-Iodohuperzine A (**3**, 0.14 mmol, 50 mg), copper(I) iodide (1 mg, 4 mol %), and K_2CO_3 (0.41 mmol, 56 mg) were charged in a 15 mL sealed screw-capped tube under air, and 5.0 mL of ethanol was added *via* a syringe. The sealed tube was closed tightly after purging with argon gas flow. The reaction mixture was heated at 140 °C and stirred for 72 h. The crude mixture was filtered through a patch of silica gel and washed with ethanol. The crude product was purified by flash column chromatography (7−15% v/v MeOH in CH_2Cl_2) to afford 2-ethoxyhuperzine A (**11**, 11 mg, 29%).

*(5R,9R,E)-5-Amino-3-ethoxy-11-ethylidene-7-methyl-5,6,9,10-tetrahydro-5,9-methanocycloocta[b]pyridin-2(1H)-one (**11**).* Yellowish solid; m.p. 104 °C; $[\alpha]_D^{26}$ −61.3° (c 1.5, CH_3OH); R_f = 0.09 (10% v/v MeOH in CH_2Cl_2); IR (neat) ν 2926, 1647, 1618, 1569, 1455, 1246 cm^{-1}; ^1H NMR (300 MHz, CD_3OD) δ_H 7.33 (s, 1H), 5.53 (q, J = 6.0 Hz, 1H), 5.45 (d, J = 6.0 Hz, 1H), 4.04 (q, J = 6.0 Hz, 2H), 3.60−3.70 (m, 1H), 2.76 (dd, J = 18.0, 6.0 Hz, 1H), 2.55 (dd, J = 18.0, 3.0 Hz, 1H), 2.27 (s, 2H), 1.72 (d, J = 6.0 Hz, 3H), 1.57 (s, 3H), 1.41 (t, J = 6.0 Hz, 3H); ^{13}C NMR (75 MHz, CD_3OD) δ_C 160.3, 148.3, 140.9, 134.8, 133.9, 125.2, 122.1, 115.7, 112.9, 65.5, 56.0, 48.8, 35.3, 34.0, 22.7, 14.8, 12.5; (+)-HRMS (ESI) m/z calcd for $C_{17}H_{23}N_2O_2$ $[M + H]^+$, 287.1754; found 287.1751.

Formation of Compound ***12*** *by Copper-Catalyzed Heteroarene Alkoxylation of 2-Iodohuperzine A (**3**).* 2-Iodohuperzine A (**3**, 0.54 mmol, 200 mg), copper(I) iodide (4 mg, 4 mol %), and K_2CO_3 (1.63 mmol, 225 mg) were charged in a 15 mL sealed screw-capped tube under air, and 5.0 mL of *n*-propanol was added *via* a syringe. The sealed tube was closed tightly after purging with argon gas flow. The reaction mixture was heated at 140 °C and stirred for 72 h. The crude mixture was filtered through a patch of silica gel and washed with *n*-propanol. The crude product was purified by flash column chromatography (7−15% v/v MeOH in CH_2Cl_2) to afford 2-propoxyhuperzine A (**12**, 107 mg, 66%).

*(5R,9R,E)-5-Amino-11-ethylidene-7-methyl-3-propoxy-5,6,9,10-tetrahydro-5,9-methanocycloocta[b]pyridin-2(1H)-one (**12**).* Yellowish solid; m.p. 109−111 °C; $[\alpha]_D^{26}$ −67.5° (c 3.2, CH_3OH); R_f = 0.26 (10% v/v MeOH in CH_2Cl_2); IR (neat) ν 2922, 1650, 1613, 1572, 1455, 1263 cm^{-1}; ^1H NMR (300 MHz, CD_3OD) δ_H 7.32 (s, 1H), 5.53 (q, J = 6.5 Hz, 1H), 5.47 (d, J = 4.2 Hz, 1H), 3.94 (t, J = 6.6, 2H), 3.60−3.69 (m, 1H), 2.76 (dd, J = 16.5, 6.0 Hz, 1H), 2.53 (dd, J = 16.5, 3.0 Hz, 1H), 2.29 (s, 2H), 1.86 (sep, J = 6.0, 2H), 1.73 (d, J = 6.0 Hz, 3H), 1.58 (s, 3H), 1.06 (t, J = 6.0 Hz, 3H); ^{13}C NMR (75 MHz, CD_3OD) δ_C 160.3, 148.5, 140.6, 134.7, 133.9, 125.2, 121.8, 115.5, 113.1, 71.6, 56.2, 48.7, 35.3, 34.0, 23.3, 22.7, 12.5, 10.8; (+)-HRMS (ESI) m/z calcd for $C_{18}H_{25}N_2O_2$ $[M + H]^+$, 301.1911; found 301.1909.

Formation of Compound ***13*** *by Copper-Catalyzed Heteroarene Alkoxylation of 2-Iodohuperzine A (**3**).* 2-Iodohuperzine A (**3**, 0.54 mmol, 200 mg), copper(I) iodide (4 mg, 4 mol %), and K_2CO_3 (1.63 mmol, 225 mg) were charged in a 15 mL sealed screw-capped tube under air, and 5.0 mL of *n*-butanol was added *via* a syringe. The sealed tube was closed tightly after purging with argon gas flow. The reaction mixture was heated at 140 °C and stirred for 72 h. The crude mixture was filtered through a patch of silica gel and washed with *n*-butanol. The crude product was purified by flash column chromatography (7−15% v/v MeOH in CH_2Cl_2) to afford 2-butoxyhuperzine A (**13**, 109 mg, 64%).

*(5R,9R,E)-5-Amino-3-butoxy-11-ethylidene-7-methyl-5,6,9,10-tetrahydro-5,9-methanocycloocta[b]pyridin-2(1H)-one (**13**).* Brownish solid; m.p. 110−111 °C; $[\alpha]_D^{26}$ −127.3° (c 1.1, CH_3OH); R_f = 0.57 (10% v/v MeOH in CH_2Cl_2); IR (neat) ν 2925, 1648, 1619, 1571, 1464, 1246 cm^{-1}; ^1H NMR (300 MHz, CD_3OD) δ_H 7.34 (s, 1H), 5.55 (q, J = 6.0 Hz, 1H), 5.43 (d, J = 3.0 Hz, 1H), 3.97 (t, J = 6.0, 2H), 3.60−3.70 (m, 1H), 2.74 (dd, J = 18.0, 6.0 Hz, 1H), 2.51 (d, J = 18.0 Hz, 1H), 2.22 (s, 1H), 2.21 (s, 1H), 1.75−1.85 (m, 2H), 1.71 (d, J = 6.0 Hz, 3H), 1.57 (s, 3H), 1.42−1.60 (m, 2H), 0.99 (t, J = 6.0 Hz, 3H); ^{13}C NMR (75 MHz, CD_3OD) δ_C 160.3, 148.4, 141.9, 135.1, 133.7, 125.2, 123.1, 116.1, 112.6, 69.7, 55.6, 49.3, 35.4, 34.1, 32.1, 22.7, 20.3, 14.2, 12.5; (+)-HRMS (ESI) m/z calcd for $C_{19}H_{27}N_2O_2$ $[M + H]^+$, 315.2067; found 315.2067.

Formation of Compound ***14*** *by O-Methylation of Huperzine A (**1**).* The mixture of HupA (**1**, 0.12 mmol, 30 mg) and Ag_2CO_3 (0.62 mmol, 171 mg) in CH_2Cl_2 (2.0 mL) was treated with iodomethane (7.43 mmol, 0.5 mL) slowly at room temperature for 45 h. The crude mixture was filtered through celite and washed with CH_2Cl_2 (10 mL). The combined organic layers were washed with sat. NaCl (5 mL), then dried over anhydrous Na_2SO_4, and concentrated under reduced pressure. The crude product was purified by flash column chromatography (2−4% v/v MeOH in CH_2Cl_2) to afford *O*-methylhuperzine A (**14**, 15 mg, 46%).

*(5R,9R,E)-11-ethylidene-2-methoxy-7-methyl-9,10-dihydro-5,9-methanocycloocta[b]pyridin-5(6H)-amine (**14**).* Clear viscous liquid; $[\alpha]_D^{26}$ −92.0° (c 1.0, CH_3OH); R_f =

https://doi.org/10.1021/acsomega.1c02875
ACS Omega 2021, 6, 19924−19939

0.40 (7% v/v MeOH in CH_2Cl_2); IR (neat) ν 2924, 1594, 1576, 1473, 1321, 1256 cm^{-1}; ^1H NMR (300 MHz, $CDCl_3$) δ_H 7.95 (d, J = 9.0 Hz, 1H), 6.57 (d, J = 9.0 Hz, 1H), 5.49 (q, J = 6.0 Hz, 1H), 5.44 (d, J = 3.0 Hz, 1H), 3.87 (s, 3H), 3.60−3.70 (m, 1H), 2.99 (dd, J = 18.0, 6.0 Hz, 1H), 2.85 (dd, J = 18.0, 3.0 Hz, 1H), 2.18 (s, 2H), 1.72 (d, J = 6.0 Hz, 3H), 1.51 (s, 3H); ^{13}C NMR (75 MHz, $CDCl_3$) δ_C 162.7, 153.6, 143.7, 136.7, 133.5, 133.0, 125.1, 110.7, 108.2, 55.4, 53.5, 50.7, 40.5, 34.0, 22.8, 12.6; (+)-HRMS (ESI) m/z calcd for $C_{16}H_{21}N_2O$ $[M + H]^+$, 257.1648; found 257.1649.

*Formation of Compounds **15**−**17** by N-Methylation of Huperzine A (**1**).* The mixture of HupA (**1**, 1.03 mmol, 250 mg) and Ag_2CO_3 (5.16 mmol, 1.42 g) in CH_2Cl_2 (5.0 mL) was treated with iodomethane (61.90 mmol, 3.9 mL) slowly at room temperature for 72 h. The crude mixture was filtered through celite and washed with CH_2Cl_2 (10 mL). The combined organic layers were washed with sat. NaCl (5 mL), then dried over anhydrous Na_2SO_4, and concentrated under reduced pressure. The crude product was purified by flash column chromatography (2−4% v/v MeOH in CH_2Cl_2) to afford *N,N,O*-trimethylhuperzine A (**15**, 56 mg, 19%), *N,N,N′*-trimethylhuperzine A (**16**, 76 mg, 26%), and *N,N*-dimethylhuperzine A (**17**, 28 mg, 10%).

*(5R,9R,E)-11-Ethylidene-2-methoxy-N,N,7-trimethyl-9,10-dihydro-5,9-methanocycloocta[b]pyridin-5(6H)-amine (**15**).* Clear viscous liquid; $[\alpha]_D^{26}$ −15.0° (c 2.0, CH_3OH); R_f = 0.80 (7% v/v MeOH in CH_2Cl_2); IR (neat) ν 2924, 1592, 1575, 1473, 1359, 1254 cm^{-1}; ^1H NMR (300 MHz, $CDCl_3$) δ_H 7.63 (d, J = 6.0 Hz, 1H), 6.51 (d, J = 6.0 Hz, 1H), 5.48 (q, J = 6.0 Hz, 1H), 5.35 (d, J = 3.0 Hz, 1H), 3.87 (s, 3H), 3.54−3.64 (m, 1H), 2.94 (dd, J = 18.0, 6.0 Hz, 1H), 2.87 (s, 3H), 2.74 (dd, J = 18.0, 3.0 Hz, 1H), 2.64 (s, 1H), 2.12 (s, 3H), 2.10 (s, 1H), 1.69 (d, J = 6.0 Hz, 3H), 1.50 (s, 3H); ^{13}C NMR (75 MHz, $CDCl_3$) δ_C 162.2, 154.2, 138.5, 137.5, 133.9, 132.5, 124.9, 113.3, 107.8, 63.3, 53.3, 47.9, 40.6, 39.9, 39.4, 34.5, 23.2, 12.5; (+)-HRMS (ESI) m/z calcd for $C_{18}H_{25}N_2O$ $[M + H]^+$, 285.1961; found 285.1959.

*(5R,9R,E)-5-(Dimethylamino)-11-ethylidene-1,7-dimethyl-5,6,9,10-tetrahydro-5,9-methanocycloocta[b]pyridin-2(1H)-one (**16**).* Clear viscous liquid; $[\alpha]_D^{26}$ −11.0° (c 2.5, CH_3OH); R_f = 0.57 (7% v/v MeOH in CH_2Cl_2); IR (neat) ν 1649, 1577, 1538, 1416 cm^{-1}; ^1H NMR (300 MHz, $CDCl_3$) δ_H 7.45 (d, J = 9.0 Hz, 1H), 6.42 (d, J = 12.0 Hz, 1H), 5.42 (q, J = 6.0 Hz, 1H), 5.28 (d, J = 3.0 Hz, 1H), 3.50−3.60 (m, 1H), 3.41 (s, 3H), 2.80 (s, 3H), 2.71 (dd, J = 15.0, 6.0 Hz, 1H), 2.64 (dd, J = 15.0, 3.0 Hz, 2H), 2.13 (s, 3H), 2.03 (d, J = 15.0 Hz, 1H), 1.63 (d, J = 9.0 Hz, 3H), 1.53 (s, 3H); ^{13}C NMR (75 MHz, $CDCl_3$) δ_C 163.4, 144.0, 138.5, 136.4, 135.3, 124.0, 123.1, 117.3, 113.9, 62.6, 46.1, 40.0, 39.2, 35.6, 33.6, 31.0, 23.0, 12.5; (+)-HRMS (ESI) m/z calcd for $C_{18}H_{25}N_2O$ $[M + H]^+$, 285.1961; found 285.1959.

*(5R,9R,E)-5-(Dimethylamino)-11-ethylidene-7-methyl-5,6,9,10-tetrahydro-5,9-methanocycloocta[b]pyridin-2(1H)-one (**17**).* Clear viscous liquid; $[\alpha]_D^{26}$ −51.4° (c 1.4, CH_3OH); R_f = 0.02 (7% v/v MeOH in CH_2Cl_2); IR (neat) ν 2923, 1654, 1614, 1459, 1260 cm^{-1}; ^1H NMR (300 MHz, $CDCl_3$) δ_H 7.57 (d, J = 9.0 Hz, 1H), 6.39 (d, J = 9.0 Hz, 1H), 5.45 (q, J = 6.0 Hz, 1H), 5.35 (s, 1H), 3.50−3.56 (m, 1H), 2.84 (s, 3H), 2.62 (d, J = 15.0 Hz, 2H), 2.20 (s, 3H), 2.02 (d, J = 18.0 Hz, 2H), 1.65 (d, J = 6.0 Hz, 1H), 1.56 (s, 3H); ^{13}C NMR (75 MHz, $CDCl_3$) δ_C 165.1, 143.6, 141.4, 137.1, 134.8, 124.2, 122.8, 117.0, 114.2, 62.4, 46.3, 40.3, 39.2, 34.9, 33.5, 23.2, 12.5; (+)-HRMS (ESI) m/z calcd for $C_{17}H_{23}N_2O$ $[M + H]^+$, 271.1805; found 271.1805.

*Formation of Compound **18** by Acetylation of Huperzine A (**1**).* Hup A **1** (0.33 mmol, 80 mg) was reacted with acetic anhydride (5.67 mmol, 532 μL) in CH_2Cl_2 (2.0 mL) at room temperature for 2 h. The reaction mixture was quenched with H_2O (10 mL) and extracted three times with CH_2Cl_2 (10 mL). The combined organic layers were washed with sat. NaCl (10 mL), then dried over anhydrous Na_2SO_4, and concentrated under reduced pressure. The crude product was purified by flash column chromatography (5% v/v MeOH in CH_2Cl_2) to afford *N*-acetylhuperzine A (**18**, 60 mg, 64%).

*N-((5R,9R,E)-11-Ethylidene-7-methyl-2-oxo-2,6,9,10-tetrahydro-5,9-methanocycloocta[b]pyridin-5(1H)-yl)acetamide (**18**).* White solid; m.p. 180 °C (decomposed); $[\alpha]_D^{26}$ +15.0° (c 1.0, CH_3OH); R_f = 0.20 (5% v/v MeOH in CH_2Cl_2); IR (neat) ν 3271, 2932, 1656, 1614, 1555, 1453, 1555, 1453, 1374, 1298, 835 cm^{-1}; ^1H NMR (400 MHz, $CDCl_3$) δ_H 7.44 (d, J = 9.5 Hz, 1H), 6.40 (d, J = 9.5 Hz, 1H), 5.43 (br s, 1H), 5.30 (q, J = 7.0 Hz, 1H), 3.60 (br s, 1H), 2.96 (dd, J = 15.0, 4.8 Hz, 1H), 2.72 (d, J = 15.0 Hz, 1H), 2.27 (d, J = 6.0 Hz, 1H), 2.23 (d, J = 6.0 Hz, 1H), 2.08 (s, 3H), 1.67 (d, J = 7.0 Hz, 3H), 1.55 (s, 3H); ^{13}C NMR (100 MHz, $CDCl_3$) δ_C 175.2, 165.1, 142.5, 139.0, 134.7, 124.8, 120.1, 118.5, 114.5, 112.8, 58.4, 49.4, 34.5, 32.6, 34.3, 22.5, 12.5; HRMS (ESI-TOF) m/z calcd for $C_{17}H_{20}N_2O_2$ $[M + H]^+$, 285.1525; found 285.1573.

*Formation of Compound **20** by Amine Protection of Huperzine A (**1**).* To an oven-dried sealed tube were added huperzine A (**1**) (0.5 mmol, 121 mg), CH_2Cl_2 (1.1 mL), and Et_3N (1.0 mmol, 0.14 mL). The reaction mixture was stirred for 5 min and cooled to 0 °C. Trifluoroacetic anhydride (1.5 equiv, 0.1 mL) was added dropwise over 5 min. The resulting mixture was allowed to warm to room temperature and stirred for 20 h. The reaction mixture was washed with sat. $NaHCO_3$(aq) (10 mL). The aqueous layer was extracted with EtOAc (10 mL). The combined organic layer was washed with brine (10 mL), dried over Na_2SO_4, and concentrated *in vacuo* to provide the crude product. The crude mixture was filtered through a patch of silica gel and washed with 10% MeOH in CH_2Cl_2 to afford *N*-triflate huperzine A (**20**, 64 mg, 38%).

*(5R,9R,E)-11-Ethylidene-7-methyl-2-oxo-5-((2,2,2-trifluoro-1,1-dioxo-1λ^7-ethoxy)amino)-1,2,5,6,9,10-hexahydro-5,9-methanocycloocta[b]pyridine (**20**).* White solid; m.p. 192−195 °C; $[\alpha]_D^{26}$ −9.6° (c 2.3, CH_3OH); R_f = 0.30 (10% v/v MeOH in CH_2Cl_2); IR(neat) ν 3217, 3026, 2908, 1728, 1651, 1612, 1550, 1453, 1186, 1151, 834, 727 cm^{-1}; ^1H NMR (400 MHz, $CDCl_3$) δ_H 7.35 (d, J = 9.5 Hz, 1H), 6.43 (d, J = 9.5, 1H), 6.31 (s, 1H), 5.45 (br s, 1H), 5.24 (q, J = 8.0 Hz, 1H), 3.64 (br. s, 1H), 2.97 (dd, J = 17.0, 5.0 Hz, 1H), 2.71 (d, J = 16.0, 1H), 2.40 (d, J = 16.0 Hz, 2H), 1.69 (d, J = 8.0 Hz, 3H), 1.58 (s, 3H); ^{13}C NMR (75 MHz, $CDCl_3$) δ_C 165.0, 155.8 (q, 144.4), 143.2, 138.2, 133.3, 132.4, 124.6, 118.2, 115.7 (q, 62.4), 113.3, 59.4, 46.9, 34.4, 32.6, 22.5, 12.5; HRMS (ESI-TOF) m/z calcd for $C_{17}H_{18}F_3N_2O_2$[M + H]$^+$, 339.1315; found 339.1312.

*Formation of Compound **21** by Amine Protection of Huperzine A (**1**).* Huperzine A (**1**) (0.21 mmol, 50 mg) was reacted with Boc_2O (1.03 mmol, 225 mg), DMAP (0.08 mmol, 10 mg), and Et_3N (0.62 mmol, 86 μL) in CH_2Cl_2 (1.0 mL) at room temperature for 1.5 h. H_2O (10 mL) was added, and the mixture was extracted three times with CH_2Cl_2 (10 mL). The combined organic layers were washed with sat. NaCl (10 mL),

https://doi.org/10.1021/acsomega.1c02875
ACS Omega 2021, 6, 19924−19939

then dried over anhydrous Na_2SO_4, and evaporated under reduced pressure. The crude product was purified by flash column chromatography (10% v/v MeOH in CH_2Cl_2) to afford *N-tert*-butyloxycarbonylhuperzine A (**21**, 20 mg, 29%).

*tert-Butyl-((5R,9R,E)-11-ethylidene-7-methyl-2-oxo-2,6,9,10-tetrahydro-5,9-methanocycloocta[b]pyridin-5(1H)-yl)carbamate (**21**).* White solid; $[\alpha]_D^{26}$ −56.4° (*c* 1.1, CH_3OH); R_f = 0.20 (10% v/v MeOH in CH_2Cl_2); IR (neat) ν 2927, 1758, 1584, 1229, 1143 cm^{-1}; ^1H NMR (300 MHz, $CDCl_3$) δ_H 8.21 (d, *J* = 9.0 Hz, 1H), 6.95 (d, *J* = 9.0 Hz, 1H), 5.52 (q, *J* = 6.0 Hz, 1H), 5.44 (d, *J* = 6.0 Hz, 1H), 3.60−3.69 (m, 1H), 3.05 (dd, *J* = 18.0, 6.0 Hz, 1H), 2.94 (dd, *J* = 18.0, 3.0 Hz, 1H), 2.22 (br s, 2H), 1.73 (d, *J* = 9.0 Hz, 3H), 1.54 (s, 9H), 1.51 (s, 3H); ^{13}C NMR (75 MHz, $CDCl_3$) δ_C 155.91, 155.57, 151.46, 142.69, 139.08, 137.66, 133.2, 125.0, 113.4, 111.5, 83.8, 55.6, 50.7, 40.1, 33.7, 27.7 (3C), 22.5, 12.5. (+)-HRMS (ESI) *m/z* calcd for $C_{20}H_{27}N_2O_3$ $[M + H]^+$, 343.2016; found 343.2018.

*Formation of Compound **22** by Bromination of N-Acetylhuperzine A (**18**).* *N*-Acetylhuperzine A (**18**) (0.07 mmol, 19 mg) was reacted with $CuBr_2$ (0.08 mmol, 19 mg) in acetonitrile (2.0 mL) under an Ar atmosphere at 50 °C for 17 days. The reaction mixture was quenched with H_2O (10 mL) and extracted three times with CH_2Cl_2 (10 mL). The combined organic layers were washed with sat. NaCl (10 mL), then dried over anhydrous Na_2SO_4, and evaporated under reduced pressure. The crude product was purified by flash column chromatography (5% v/v MeOH in CH_2Cl_2) to afford 2-bromo-*N*-acetylhuperzine A (**22**, 21 mg, 86%).

*N-((5R,9R,E)-3-Bromo-11-ethylidene-7-methyl-2-oxo-2,6,9,10-tetrahydro-5,9-methanocycloocta[b]pyridin-5(1H)-yl)acetamide (**22**).* Pale yellow solid; m.p. 180 °C (decomposed); $[\alpha]_D^{26}$ −29.0° (*c* 4.2, CH_3OH); R_f = 0.70 (5% v/v MeOH in CH_2Cl_2); IR (neat) ν 3282, 2929, 1646, 1616, 1548, 1450, 1377, 1294, 1258, 1024, 952, 789, 735 cm^{-1}; ^1H NMR (400 MHz, $CDCl_3$) δ_H 7.74 (s, 1H), 5.45 (d, *J* = 4.8 Hz, 1H), 5.29 (q, *J* = 6.8 Hz, 1H), 3.63 (br s, 1H), 2.93 (dd, *J* = 5.6, 4.4 Hz, 1H), 2.63 (d, *J* = 15.6 Hz, 1H), 2.21 (d, *J* = 12.0 Hz, 1H), 2.11 (s, 1H), 2.08 (s, 3H), 1.60 (d, *J* = 6.8 Hz, 3H), 1.56 (s, 3H); ^{13}C NMR (100 MHz, $CDCl_3$) δ_C 167.7, 159.7, 141.1, 139.7, 132.7, 131.4, 123.8, 119.9, 112.3, 57.0, 33.3, 31.5, 29.1, 23.2, 21.5, 21.4, 11.5; HRMS (ESI-TOF) *m/z* calcd for $C_{17}H_{20}{}^{79}BrN_2O_2$ $[M + H]^+$, 363.0630; found 363.0703.

*Formation of Compound **23** by Iodination of N-Acetylhuperzine A (**18**).* *N*-Acetylhuperzine A (**18**) (0.11 mmol, 28 mg) was reacted with NIS (0.17, 15 mg) in CH_2Cl_2 (1.0 mL) at room temperature for 5.5 h. The reaction mixture was quenched with H_2O (10 mL) and extracted three times with CH_2Cl_2 (10 mL). The combined organic layers were washed with sat. NaCl (10 mL), then dried over anhydrous Na_2SO_4, and evaporated under reduced pressure. The crude product was purified by flash column chromatography (7% v/v MeOH in CH_2Cl_2) to afford 2-iodo-*N*-acetylhuperzine A (**23**, 20 mg, 45%).

*N-((5R,9R,E)-11-Ethylidene-3-iodo-7-methyl-2-oxo-2,6,9,10-tetrahydro-5,9-methanocycloocta[b]pyridin-5(1H)-yl)acetamide (**23**).* Pale yellow solid; m.p. 200 °C (decomposed); $[\alpha]_D^{26}$ −97.5° (*c* 3.2, CH_3OH); R_f = 0.40 (5% v/v MeOH in CH_2Cl_2); IR (neat) ν 3277, 3049, 2926, 2858, 1636, 1612, 1542, 1423, 1264, 1182, 732,7014, cm^{-1}; ^1H NMR (400 MHz, $CDCl_3$) δ_H 7.89 (s, 1H), 5.46 (d, *J* = 8.4 Hz, 1H), 5.22 (q, *J* = 8.8 Hz, 1H), 3.50 (t, *J* = 4.0 Hz, 1H), 2.85 (dd, *J* = 12.8, 4.4 Hz, 1H), 2.55 (d, *J* = 16.8 Hz, 1H), 2.19 (s, 1H), 2.08 (s, 3H), 1.60 (d, *J* = 6.8 Hz, 3H), 1.51 (s, 3H); ^{13}C NMR (100 MHz, $CDCl_3$) δ_C 169.0, 161.8, 147.5, 143.4, 134.0, 132.5, 124.8, 123.0, 113.3, 58.0, 47.8, 34.4, 32.5, 29.7, 24.3, 22.5, 12.5; HRMS (ESI-TOF) *m/z* calcd for $C_{17}H_{20}{}^{127}IN_2O_2$ $[M + H]^+$, 411.0564; found 411.0562.

Biological Studies. *AChE and BChE Inhibition Assays.* The AChE inhibition activity of HupA derivatives were measured using the spectrometric method of Ellman.[48] Briefly, 20 μL of the tested compound solution (dissolved in methanol with DMSO as a solubilizing agent), 100 μL of phosphate buffer (pH 8.0), and 20 μL of 3.3 mM 5,5′-dithiobis-2-nitrobenzoic acid (DTNB) aqueous solution were transferred into a 96-well plate. A total of 40 μL of 0.25 U/mL electric eel acetylcholinesterase (*ee*AChE, Sigma-Aldrich) solution was added into the mixture and incubated at 37 °C for 20 min. After incubation, 20 μL of 5 mM acetylthiocholine iodide (ATCI) was added and shaken gently. The absorbance was measured at 412 nm every 20 s for 3 min using a microplate reader with a UV−visible spectrometer to obtain the enzymatic reaction rate (maximal velocity, V_{max}). Phosphate buffer (pH 8.0) instead of AChE was used as the blank to obtain the enzymatic reaction rate of the blank (V_{blank}). Donepezil hydrochloride monohydrate instead of the tested compound was used as the positive control, and methanol was used as the negative control ($V_{control}$).

The percentage inhibition activity of AChE of all HupA analogs was calculated using the following equation:

$$\%\text{inhibition} = \frac{(V_{control} - V_{blank}) - (V_i - V_{blank})}{(V_{control} - V_{blank})} \times 100$$

where $V_{control}$ = enzymatic reaction rate of control, V_{blank} = enzymatic reaction rate of blank, and V_i = enzymatic reaction rate of tested compound.

The inhibition activities of AChE of all HupA analogs were expressed as the half-maximal inhibitory concentration (IC_{50}) using 8−10 different concentrations of each HupA analog. The compounds with IC_{50} concentration more than 1000 μM was considered as inactive. All determinations were carried out in triplicate and expressed as mean ± standard error of the mean (S.E.M.). For the BChE inhibition assay, experimental procedures and calculations of the BChE inhibition activity of HupA analogs were conducted similar to the methods described previously, but using butyrylthiocholine iodide (BTCI) instead of ATCI and BChE from equine serum (*eq*-BChE) instead of *ee*AChE.

Cell Culture. The normal human lung fibroblast cell line (IMR90) was purchased from the American Type Culture Collection (ATCC; Manassas, VA, USA). Cells were cultured in DMEM (Dulbecco's Modified Eagle's Medium) supplemented with 10% fetal bovine serum, 100 U/mL penicillin, and 100 μg/mL streptomycin. Cells were maintained under 5% CO_2 at 37 °C in humidified air.

MTT Assay. IMR90 cells were plated into 96-well plates at a density of 5×10^4 cells/well. After 18 h of incubation, the tested samples at the indicated concentrations were added into triplicate wells. Cells were then incubated for 24 h. The cell viability was determined using the MTT (3-(4,5-dimethylthiazol-2-yl)-2,5-diphenyltetrazolium bromide) assay. Briefly, the supernatant was removed. A total of 100 μL of the MTT solution (0.5 mg MTT in 1.0 mL complete medium) was added to each well. The cells were incubated at 37 °C for 3 h. The solution was then replaced with 100 μL of DMSO. The

https://doi.org/10.1021/acsomega.1c02875
ACS Omega 2021, 6, 19924−19939

absorbance was measured at 570 nm using a microplate reader (Modular multimode microplate reader, Thermo Scientific). % Cytotoxicity was calculated by comparing the absorbance of the treated wells to the untreated control according to the following equation: %Cytotoxicity = [1 − [Abs (sample)/Abs (untreated control)]] × 100. The experiment was done in triplicate.

Data Analysis and Statistical Methods. The data from the experiment was expressed as mean ± standard error of mean (S.E.M). One-way ANOVA and post hoc least-significant difference (LSD) were used to determine the statistical significance of the difference between groups. The association between the estimated K_i value according to the docking program and calculated K_i according to *in vitro* results used Pearson and Spearman's correlation analysis. $p < 0.05$ was considered statistically significant.

■ ASSOCIATED CONTENT

Supporting Information

The Supporting Information is available free of charge at https://pubs.acs.org/doi/10.1021/acsomega.1c02875.

> Preliminary *in silico* study by using BUDE docking, BUDE docking analysis of preselected huperzine A analogs against *h*AChE, physiochemical properties of preselected C(2) huperzine A analogs, synthesis of *N*-protected HupA derivatives **18**−**23**, complete ^{1}H and ^{13}C NMR spectroscopic data of selected C(2) huperzine A and compounds **2**−**23** (PDF)

■ AUTHOR INFORMATION

Corresponding Author

Nopporn Thasana − *Program in Chemical Sciences, Chulabhorn Graduate Institute, Chulabhorn Royal Academy, Bangkok 10210, Thailand; Laboratory of Medicinal Chemistry, Chulabhorn Research Institute, Bangkok 10210, Thailand; The Center of Excellence on Environmental Health and Toxicology, Commission on Higher Education, Ministry of Education, Bangkok 10400, Thailand;* orcid.org/0000-0002-0572-4871; Phone: +66-2-574-0622; Email: nopporn@cri.or.th; Fax: +66-2-574-2027

Authors

Shisanupong Anukanon − *Program in Chemical Sciences, Chulabhorn Graduate Institute, Chulabhorn Royal Academy, Bangkok 10210, Thailand*

Pornkanok Pongpamorn − *Program in Chemical Sciences, Chulabhorn Graduate Institute, Chulabhorn Royal Academy, Bangkok 10210, Thailand;* Present Address: Present address: National Omics Center, National Science and Technology Development Agency, Pathum Thani 12120, Thailand (P.P.)

Wareepat Tiyabhorn − *Program in Chemical Sciences, Chulabhorn Graduate Institute, Chulabhorn Royal Academy, Bangkok 10210, Thailand*

Jaruwan Chatwichien − *Program in Chemical Sciences, Chulabhorn Graduate Institute, Chulabhorn Royal Academy, Bangkok 10210, Thailand*

Worawat Niwetmarin − *Program in Chemical Sciences, Chulabhorn Graduate Institute, Chulabhorn Royal Academy, Bangkok 10210, Thailand*

Richard B. Sessions − *School of Biochemistry, University of Bristol, Bristol BS8 1TD, United Kingdom;* orcid.org/0000-0003-0320-0895

Somsak Ruchirawat − *Program in Chemical Sciences, Chulabhorn Graduate Institute, Chulabhorn Royal Academy, Bangkok 10210, Thailand; Laboratory of Medicinal Chemistry, Chulabhorn Research Institute, Bangkok 10210, Thailand; The Center of Excellence on Environmental Health and Toxicology, Commission on Higher Education, Ministry of Education, Bangkok 10400, Thailand*

Complete contact information is available at: https://pubs.acs.org/10.1021/acsomega.1c02875

Funding

This research project was supported by the Center of Excellence on Environmental Health and Toxicology (EHT), the Thailand Research Fund, and Thailand Science Research and Innovation.

Notes

The authors declare no competing financial interest.

■ ACKNOWLEDGMENTS

This work was partially supported by the Thailand Research Fund (BRG6080013 for N.T.), Thailand Science Research and Innovation Grant number FEB640035 Project code 50184 for Chulabhorn Royal Academy. Support from the Center of Excellence on Environmental Health and Toxicology, Science & Technology Postgraduate Education and Research Development Office (PERDO), Ministry of Education is also gratefully acknowledged. The authors thank Prof. Timothy C. Gallagher, University of Bristol, UK, for valuable comments on the manuscript.

■ REFERENCES

(1) Querfurth, H. W.; LaFerla, F. M. Alzheimer's disease. *N. Engl. J. Med.* **2010**, *362*, 329−344.

(2) GBD 2019 Diseases and Injuries Collaborators. Global burden of 369 diseases and injuries in 204 countries and territories, 1990-2019: a systematic analysis for the Global Burden of Disease Study 2019. *Lancet* **2020**, *396*, 1204−1222.

(3) Alzheimer's Disease International (ADI). *World Alzheimer Report 2019: Attitudes to Dementia*. London, England: Alzheimer's Disease International (ADI), 2019.

(4) Chen, X. Q.; Mobley, W. C. Exploring the Pathogenesis of Alzheimer Disease in Basal Forebrain Cholinergic Neurons: Converging Insights From Alternative Hypotheses. *Front. Neurosci.* **2019**, *13*, 1−18.

(5) Giacobini, E. Cholinergic Function and Alzheimer's Disease. *Int. J. Geriatr. Psychiatry.* **2003**, *18*, S1−S5.

(6) Masters, C. L.; Bateman, R.; Blennow, K.; Rowe, C. C.; Sperling, R. A.; Cummings, J. L. Alzheimer's disease. *Nat. Rev. Dis. Primers.* **2015**, *1*, 1−18.

(7) Lockridge, O. Review of Human Butyrylcholinesterase Structure, Function, Genetic Variants, History of Use in the Clinic, and Potential Therapeutic Uses. *Pharmacol. Ther.* **2015**, *148*, 34−46.

(8) Reiner, E.; Radič, Z. Mechanism of action of cholinesterase inhibitors. In *Cholinesterases and Cholinesterase Inhibitors*; Giacobini, E, ed.; Martin Dunitz: London, 2000, 103−20.

(9) Yan, J.; Sun, L.; Wu, G.; Yi, P.; Yang, F.; Zhou, L.; Zhang, X.; Li, Z.; Yang, X.; Luo, H.; Qiu, M. Rational Design and Synthesis of Highly Potent Anti-Acetylcholinesterase Activity Huperzine A Derivatives. *Bioorg. Med. Chem.* **2009**, *17*, 6937−6941.

(10) Ferreira, A.; Rodrigues, M.; Fortuna, A.; Falcão, A. Alves. Huperzine A from *Huperzia serrata*: a review of its sources, chemistry, pharmacology and toxicology. *Phytochem. Rev.* **2006**, *15*, 51−85.

(11) Yue, J.; Dong, B. R.; Lin, X.; Yang, M.; Wu, H. M.; Wu, T. Huperzine A for mild cognitive impairment. *Cochrane Database Syst. Rev.* **2012**, *12*, CD008827.
(12) Yang, G.; Wang, Y.; Tian, J.; Liu, J. P. Huperzine A for Alzheimer's disease: a systematic review and meta-analysis of randomized clinical trials. *PLoS One* **2013**, *8*, No. e74916.
(13) Nilsu, T.; Thorroad, S.; Ruchirawat, S.; Thasana, N. Squarrosine A and pyrrolhuperzine A, New *Lycopodium* Alkaloids from Thai and Philippine *Huperzia squarrosa*. *Planta Med.* **2016**, *82*, 1046−1050.
(14) Thorroad, S.; Worawittayanont, P.; Khunnawutmanotham, N.; Chimnoi, N.; Jumruksa, A.; Ruchirawat, S.; Thasana, N. Three New *Lycopodium* Alkaloids from *Huperzia carinata* and *Huperzia squarrosa*. *Tetrahedron* **2014**, *70*, 8017−8022.
(15) Nilsu, T.; Thaisaeng, W.; Thamnarak, W.; Eurtivong, C.; Jumraksa, A.; Thorroad, S.; Thasana, N. Three *Lycopodium* alkaloids from Thai club mosses. *Phytochemistry* **2018**, *156*, 83−88.
(16) McIntosh-Smith, S.; Wilson, T.; Ibarra, A. A.; Crisp, J.; Sessions, R. B. Benchmarking energy efficiency, power costs and carbon emissions on heterogeneous systems. *J. Comput.* **2012**, *55*, 192−205.
(17) Cheung, J.; Rudolph, M. J.; Burshteyn, F.; Cassidy, M. S.; Gary, E. N.; Love, J.; Height, J. J. Structures of human acetylcholinesterase in complex with pharmacologically important ligands. *J. Med. Chem.* **2012**, *55*, 10282−10286.
(18) Gunosewoyo, H.; Tipparaju, S. K.; Pieroni, M.; Wang, Y.; Doctor, B. P.; Nambiar, M. P.; Kozikowski, A. P. Structural Analogs of Huperzine A Improve Survival in Guinea Pigs Exposed to Soman. *Bioorg. Med. Chem. Lett.* **2013**, *23*, 1544−1547.
(19) Camps, P.; Muñoz-Torrero, D.; Simon, M. Easy Access to 4-Substituted (±)-Huperzine a Analogues. *Synth. Commun.* **2001**, *31*, 3507−3516.
(20) Darrouzain, F.; André, C.; Ismaili, L.; Matoga, M.; Guillaume, Y. C. Huperzine A–Human Serum Albumin Association: Chromatographic and Thermodynamic Approach. *J. Chromatogr. B. Analyt. Technol. Biomed. Life Sci.* **2005**, *820*, 283−288.
(21) Kozikowski, A. P.; Ding, Q.; Saxena, A.; Doctor, B. P. Synthesis of (±)-10,10-Dimethylhuperzine A-a Huperzine Analogue Possessing a Slower Enzyme off-Rate. *Bioorg. Med. Chem. Lett.* **1996**, *6*, 259−262.
(22) Kozikowski, A. P.; Campiani, G.; Sun, L.-Q.; Wang, S.; Saxena, A.; Doctor, B. P. Identification of a More Potent Analogue of the Naturally Occurring Alkaloid Huperzine A. Predictive Molecular Modeling of Its Interaction with AChE. *J. Am. Chem. Soc.* **1996**, *118*, 11357−11362.
(23) Kozikowski, A. P.; Xia, Y.; Reddy, E. R.; Tuckmantel, W.; Hanin, I.; Tang, X. C. Synthesis of Huperzine A, Its Analogs, and Their Anticholinesterase Activity. *J. Org. Chem.* **1991**, *56*, 4636−4645.
(24) Campiani, G.; Kozikowski, A. P.; Wang, S.; Ming, L.; Nacci, V.; Saxena, A.; Doctor, B. P. Synthesis and Anticholinesterase Activity of Huperzine A Analogues Containing Phenol and Catechol Replacements for the Pyridone Ring. *Bioorg. Med. Chem. Lett.* **1998**, *8*, 1413−1418.
(25) Morris, G. M.; Huey, R.; Lindstrom, W.; Sanner, M. F.; Belew, R. K.; Goodsell, D. S.; Olson, A. J. Autodock 4 and AutoDockTools4: Automated Docking with Selective Receptor Flexibility. *J. Comput. Chem.* **2009**, *30*, 2785−2791.
(26) Pettersen, E. F.; Goddard, T. D.; Huang, C. C.; Couch, G. S.; Greenblatt, D. M.; Meng, E. C.; Ferrin, T. E. UCSF Chimera–a Visualization System for Exploratory Research and Analysis. *J. Comput. Chem.* **2004**, *25*, 1605−1612.
(27) Lipinski, C. A. Lead- and Drug-like Compounds: The Rule-of-Five Revolution. *Drug Discovery Today: Technol.* **2004**, *1*, 337−341.
(28) Clark, D. E. Rapid Calculation of Polar Molecular Surface Area and Its Application to the Prediction of Transport Phenomena. 2. Prediction of Blood-Brain Barrier Penetration. *J. Pharm. Sci.* **1999**, *88*, 815−821.
(29) Ogura, H.; Kosasa, T.; Kuriya, Y.; Yamanishi, Y. Comparison of Inhibitory Activities of Donepezil and Other Cholinesterase Inhibitors on Acetylcholinesterase and Butylcholinesterase *in Vitro*. *Methods Find. Exp. Clin. Pharmacol.* **2000**, *22*, 609.
(30) Daina, A.; Michielin, O.; Zoete, V. SwissADME: A Free Web Tool to Evaluate Pharmacokinetics, Drug-Likeness and Medicinal Chemistry Friendliness of Small Molecules. *Sci. Rep.* **2017**, *7*, 1−13.
(31) Aljamali, N. M. Review in Functional and Protecting Groups. *Int. J. Appl. Pharm. Biol. Res.* **2015**, *1*, 75−86.
(32) Greene, T. W.; Wuts, P. G. M. *Protective Groups in Organic Synthesis*; John Wiley & Sons, Inc.: New York, USA, 1999, DOI: 10.1002/0471220574.
(33) Oosthoek-de Vries, A. J.; Nieuwland, P. J.; Bart, J.; Koch, K.; Janssen, J. W. G.; van Bentum, P. J. M.; Rutjes, F. P. J. T.; Gardeniers, H. J. G. E.; Kentgens, A. P. M. Inline Reaction Monitoring of Amine-Catalyzed Acetylation of Benzyl Alcohol Using a Microfluidic Stripline Nuclear Magnetic Resonance Setup. *J. Am. Chem. Soc.* **2019**, *141*, 5369−5380.
(34) Barrett, A. G. M.; Lana, J. C. A. Selective Acylation of Amines Using 18-Crown-6. *J. Chem. Soc., Chem. Commun.* **1978**, *11*, 471−472.
(35) Baker, T. J.; Tomioka, M.; Goodman, M. Preparation and Use of *N,N′*-Di-Boc-*N″*-Triflylguanidine: Carbamic Acid, [[(Trifluoromethyl)Sulfonyl]Carbonimidoyl]Bis-, Bis(1,1-Dimethylethyl) Ester. *Org. Synth.* **2002**, *78*, 91.
(36) Flynn, D. L.; Zelle, R. E.; Greico, P. A. A Mild Two-step Method for the Hydrolysis/Methanolysis of Secondary Amides and Lactams. *Tetrahedron Lett.* **1983**, *48*, 2024−2426.
(37) Carato, P.; Yous, S.; Sellier, D.; Poupaert, J. H.; Lebegue, N.; Berthelot, P. Efficient and Selective Deprotection Method for *N*-Protected 2(3H)-Benzoxazolones and 2(3H)-Benzothiazolones. *Tetrahedron* **2004**, *60*, 10321−10324.
(38) Samanta, R. C.; Yamamoto, H. Selective Halogenation Using an Aniline Catalyst. *Chem. − Eur. J.* **2015**, *21*, 11976−11979.
(39) Sharma, K. K.; Patel, D. I.; Jain, R. Metal-Free Synthesis of N-Fused Heterocyclic Iodides *via* C-H Functionalization Mediated by Tert-Butylhydroperoxide. *Chem. Commun.* **2015**, *51*, 15129−15132.
(40) Joule, J. A.; Mills, K. *Heterocyclic Chemistry*, 5th ed.; Wiley-Blackwell: Chichester, England, 2010.
(41) Boursalian, G. B.; Ritter, T. Palladium-Mediated Fluorination for Preparing Aryl Fluorides. In *Fluorination*; Springer Singapore: Singapore, 2018; pp. 1−17.
(42) Malhotra, S.; Seng, P. S.; Koenig, S. G.; Deese, A. J.; Ford, K. A. Chemoselective Sp2-Sp3 Cross-Couplings: Iron-Catalyzed Alkyl Transfer to Dihaloaromatics. *Org. Lett.* **2013**, *15*, 3698−3701.
(43) Herbert, J. M. Negishi-Type Coupling of Bromoarenes with Dimethylzinc. *Tetrahedron Lett.* **2004**, *45*, 817−819.
(44) Ding, K.; Wang, D.; Kuang, L.; Li, Z. L-Proline-Promoted Rosenmund-von Braun Reaction. *Synlett* **2008**, *2008*, 69−72.
(45) Takagi, M.; Watanabe, A.; Murata, S.; Takita, R. Copper-Catalyzed Arene Amination in Pure Aqueous Ammonia. *Org. Biomol. Chem.* **2019**, *17*, 1791−1795.
(46) White, J. D.; Li, Y.; Kim, J.; Terinek, M. A Novel Synthesis of (−)-Huperzine A *via* Tandem Intramolecular Aza-Prins Cyclization-Cyclobutane Fragmentation. *Org. Lett.* **2013**, *15*, 882−885.
(47) Atri, A. Current and Future Treatments in Alzheimer's Disease. *Semin. Neurol.* **2019**, *39*, 227−240.
(48) Weinstock, M. Selectivity of Cholinesterase Inhibition: Clinical Implications for the Treatment of Alzheimer's Disease. *CNS Drugs* **1999**, *12*, 307−323.
(49) Ellman, G. L.; Courtney, K. D.; Andres, V., Jr.; Feather-Stone, R. M. A new and rapid colorimetric determination of acetylcholinesterase activity. *Biochem. Pharmacol.* **1961**, *7*, 88−95.
(50) Qian, Z. M.; Ke, Y. Huperzine A: Is It an Effective Disease-Modifying Drug for Alzheimer's Disease? *Front. Aging. Neurosci.* **2014**, *6*, 1−6.
(51) Cer, R. Z.; Mudunuri, U.; Stephens, R.; Lebeda, F. J. IC_{50}-to-K_i: A Web-Based Tool for Converting IC_{50} to K_i Values for Inhibitors of Enzyme Activity and Ligand Binding. *Nucleic Acids Res.* **2009**, *37*, W441−W445.

https://doi.org/10.1021/acsomega.1c02875
ACS Omega 2021, 6, 19924−19939